Wayne State University
DigitalCommons@WayneState

Wayne State University Theses

1-1-2010

Analysis And Evaluation Of A Vibro-Acoustic Metamaterial

Md Tofiqul Islam
Wayne State University

Follow this and additional works at: http://digitalcommons.wayne.edu/oa_theses

Recommended Citation
Islam, Md Tofiqul, "Analysis And Evaluation Of A Vibro-Acoustic Metamaterial" (2010). *Wayne State University Theses.* Paper 62.

This Open Access Embargo is brought to you for free and open access by DigitalCommons@WayneState. It has been accepted for inclusion in Wayne State University Theses by an authorized administrator of DigitalCommons@WayneState.

ANALYSIS AND EVALUATION OF A VIBRO-ACOUSTIC METAMATERIAL

by

MD. TOFIQUL ISLAM

THESIS

Submitted to the Graduate School

of Wayne State University

Detroit, Michigan

in partial fulfillment of the requirements

for the degree of

MASTER OF SCIENCE

2011

MAJOR: MECHANICAL ENGINEERING

Approved by:

_____

Advisor Date

© COPYRIGHT BY

MD TOFIQUL ISLAM

2011

All Rights Reserved

DEDICATION

To my wife Korobi Basher

ACKNOWLEDGEMENTS

I recall with sincere gratitude my supervisor Golam M. Newaz, Professor, Department of Mechanical Engineering, Wayne State University, who has guide me by his constructive suggestions and criticism to the improvement of this research work.

I owe a debt of gratitude to Korobi Basher and Dr. Mohammad Hailat who have assisted me in present research works. Special thanks also go to all of my colleagues and friends. Funding of this work was provided through Institute for Manufacturing Research (IMR) at Wayne State University and the Office of Vice President of Research (OVPR) from January 2009 to May 2010.

TABLE OF CONTENTS

DEDICATION ii

ACKNOWLEDGEMENTS iii

LIST OF TABLES ..... v i

LIST OF FIGURES vii

CHAPTER 1 : Introduction to metamaterial 1

1.1 General 1

1.2 Electro – magnetic metamaterial 2

1.3 Photonic metamaterial 2

1.4 Helmholtz Resonators 3

1.5 Objective 4

1.6 Application 5

CHAPTER 2 : Literature Review 6

CHAPTER 3 : Theory 10

3.1 Sound Propagation in Stationary Cavity Flow ... 10

3.2 Rayleigh Damping 11

CHAPTER 4 : Design and Fabrication 13

4.1 Physical Model 13

CHAPTER 5 : Experimental Analysis 17

5.1 Experimental Setup 17

5.2 Experimental Results 18

5.3 Evaluation of Rayleigh Damping Parameters 21

CHAPTER 6 : Mathematical Modeling 24

6.1 Governing Equations 24

6.2 Boundary Conditions 25

CHAPTER 7 : Computational Details 26

7.1 General 26

7.2 Finite Element Method 28

7.3 Mesh Generation 29

7.4 Convergence Test 31

7.5 Algorithm 32

7.6 Solutions of systems of equations 33

CHAPTER 8 : Numerical Analysis 38

CHAPTER 9 : Conclusion 46

REFERENCES 47

ABSTRACT 51

AUTOBIOGRAPHICAL STATEMENT 53

LIST OF TABLES

Table 4.1 Material Properties of the complex structure 16

Table 8.1 Close agreement between experiment and computation 38

LIST OF FIGURES

Figure 4.1 Physical Model 13

Figure 4.2 Design parameters of the vibro-acoustic metamaterial (a) square masses with stems, (b) top view, (c) front view and (d) LHS vies 14

Figure 5.1 Schematic diagram of experimental setup 17

Figure 5.2 Transient response of acoustic metamaterial (a) square of velocity profile and (b) impulse force 19

Figure 5.3 (a) Magnitude plot of transfer function, (b) phase plot of transfer function and (c) line spectrum of impulse force 20

Figure 5.4 Variation of damping ratio with natural frequency 21

Figure 5.5 Asymptotic nature of effective mass near natural frequencies 23

Figure 5.6 Influence of higher order natural frequencies on effective mass 23

Figure 7.1 Finite element discretization of a domain 30

Figure 7.2 Current mesh structure with 231843 numbers of nodes for acoustic cavity problem 30

Figure 8.1 Frequency response of the complex structure 37

Figure 8.2 Comparison of kinetic energy per unit mass at source and target points 38

Figure 8.3 Variation of elastic modulus of complex structure over wide range of frequencies 39

Figure 8.4 Participation of square masses attached with stems for energy absorption 40

Figure 8.5 Displacement along x-direction and deformation of internal masses with stems and complex structure 41

CHAPTER 1
INTRODUCTION

1.1 GENERAL

Veselago's [1] postulation of electro-magnetic left-handed material in 1968 did not stimulate much interest among the researches at that time. After 33 years of that concept, Pendry [2] first proposed the theoretical possibility of making electro-magnetic metamaterial which recently has many applications in superlens, cloaking device and metamaterial antennas. Out of the concept of electro-magnetic left-handed material, the concepts of negative effective modulus and negative effective mass density of acoustic metamaterial are developed by Fang et al. [3] and Huang et al. [4] respectively. However, the dispersion attributions of sound wave propagation through a tunnel with an array of Helmholtz resonators developed by Sugimoto and Horioka [5] is the base of the research work of N. Fung et al. [3] where they have developed one dimensional ultrasonic metamaterial which can create a certain band gap at near 30 kHz of its resonance. The structural dimensions of the ultrasonic metamaterial play the key role in wave attenuation for certain frequencies near its resonances. Milton and Willis [6] proposed a modified law of motion which has small difference with the Newton's second law of motion in many cases, but has enormous difference in specially designed composite materials. It is argued that these new set of equations which govern the behavior of the average weighted displacement field, may apply to all physical materials, not just

composites. Huang et al. [4] have developed their theoretical background for acoustic metamaterial which is the extension of Milton's research work. They developed an equivalent model to represent a lattice system comprising of mass - in - mass units. They concluded that the classical continuum mechanics may describe the negative effective mass density of the acoustic metamaterial. However, this theoretical system has complicacy to build experimental system which must obey the rule of left-handed acoustic metamaterial.

1.2 ELECTRO-MAGNETIC METAMATERIAL

The electromagnetic left-handed (meta) material has negative real values of permittivity and permeability. The poynting vector of a monochromatic plane wave is directed opposite to the direction of its phase velocity. Hence it supports backward wave propagation and its negative refractive index in isotropic medium. Moreover, it is constructed as a composite medium by placing arrays of small metallic wires and split – ring resonators which exhibit negative refraction in microwave regime. The electromagnetic metamaterial affects electromagnetic waves by having structural Split – Ring Resonators (SRR) or Artificial Magnetic Conductors (AMC) or High Impedance Surfaces (HIS) smaller than the wavelength of electromagnetic wave.

1.3 PHOTONIC METAMATERIAL

Photonic metamaterial, a genre of electromagnetic metamaterial, is comprised of periodic optical nanostructures that are designed to affect

the motion of photons in a same way that periodic semiconductors do for the motion of electrons. It creates forbidden electron energy bands while it is propagating through regularly repeated internal regions of high and low dielectric property. The periodic structure is much smaller than the wavelength of source. The period of sub-wavelength of the photonic metamaterial is so discernible that it separates the photonic metamaterial from photonic band gap or photonic crystals. Each periodic structural cell, designed with some specific parameters which create a shield for certain frequencies of the radiated source, is altogether represented as effective medium for optical cloaking.

1.4 HELMHOLTZ RESONANCE

Helmholtz resonance is one of the emerging branches of physics of acoustic which describes the phenomenon of air resonance in a cavity. When air inside a cavity with narrow open neck is subjected to external loading, a surge of air pressure, developed within the cavity, derives the air out through the narrow neck so rigorously that it creates lower pressure inside the cavity. Therefore, the mass of air along the narrow neck demonstrates oscillating behavior. An acoustic system tends to absorb more energy when its frequency becomes closer to its resonance frequency. It will probably have more than one resonance frequencies at which it vibrates easily compared to its other frequencies. Therefore, it attenuates almost all frequencies other than its resonances.

1.5 OBJECTIVE

In the present thesis, the vibro – acoustic metamaterial has been designed and fabricated in meso – scale which exhibits negative effective mass density and negative effective elastic modulus at its resonance frequencies. The experimental free – free vibration test has been conducted for measuring negative effective mass density of the complex structure. Moreover, the negative effective elastic modulus of the complex designed structure has been evaluated numerically. This new concept of acoustic metamaterial has the combination of two effects: dispersion property due to negative effective elastic modulus and attenuation property due to negative effective mass density resulted from the dynamic cantilever action of the metallic alloy stems with attached mass at the top. These stems are fixed at base in such a fashion that they create an array of localized resonators.

The technique for measuring negative effective elastic modulus of the acoustic metamaterial is the primary goal. The effective elastic modulus demonstrates the stresses, developed due to wave propagation as a result of repeated loading or impact loading, lead the strains at some range of phase angles. This phenomena cause the creation of stop band for certain range of frequencies which resist the incoming wave to propagate throughout the system due to the system's dispersion and attenuation properties which come from the visco-elastic system and the reciprocating action of the mass with stems at its resonance frequency

respectively. Free vibration testing with an impact hammer of 50 lbf pk and accelerometers of ± 50 g pk has been performed on the designed system. The responses of reference point and target point have been collected in terms of displacement by spectral dynamics frequency analyzer ranging from 0 to 20 kHz.

1.6 APPLICATIONS

The potential applications of the negative elastic modulus of vibro-acoustic metamaterial in naval ship design are to eliminate hydrodynamic loadings due to shock waves, weather collisions and groundings. Several thin layers of acoustic metamaterial with visco-elastic property in hull design may do good damping compared to Aluminum structure. Even the concept of dynamic localized resonator can be applicable to metallic structure by considering the cantilever action of mass with stems only.

CHAPTER 2
LITERATURE REVIEW

Cantrell and Hart [7] investigated the neutral acoustic stability condition in cavities with a transpiring wall without acoustic disturbances in case of sound and flow interaction inside acoustic cavity. They found that the growth rates and neutral stability may be expressed in terms of only first – order quantities. Soize [8] developed adaptive reduced method for structure – acoustic interaction in three-dimensional anisotropic, inhomogeneous, visco-elastic cavities for medium frequency range. The coupling between the structure of medium frequency range and acoustic of low frequency range and the coupling between structure of medium frequency range and acoustic of medium frequency range were validated. Esteve and Johnson [9] studied numerically the attenuation of sound transmission into a circular cylindrical enclosure, with distributed vibration absorbers and Helmholtz resonators, excited by an external plane wave. They concluded that the sound transmission in an enclosure has been significantly reduced as long as the structures and the cavities are lightly damped, which is usually the case at low frequency in aerospace applications. Hepberger et al. [10] validated wave based technique over finite element method for analyzing multi – domain 3D acoustic cavity with interior damping and loudspeaker excitation. Kung and Singh [11] proposed an experimental technique to identify modal parameters including damping of a three dimensional cavity. Their work was significant for diagnosing the acoustics of irregular shaped

cavities. Wang and Bathe [12] developed an effective displacement – pressure finite element formulation that satisfies inf – sup condition for the analysis of acoustic fluid – structure interaction problems.

The concept of metamaterial comes from EM theorem. Many research works have been conducted on photonic, optical and EM metamaterials which have potential existing applications. Li et al. [13] designed and simulated all dimensional sub –wavelength cavities to break the size restriction for electromagnetic metamaterial. Li et al. [14] studied on a metamaterial substrate consisting of a quasi – periodic metallic planar and a flat metal sheet, interconnected through metallic vias. They reported that this structure has multiple in-phase reflection frequency regimes and frequency band gap for transverse – magnetic surface waves whereas the transverse electric surface waves are suppressed in all frequencies. Genov et al. [15] developed an analogy of celestial mechanism in photonic metamaterial.

Huang et al. [4] demonstrated mathematically the negative mass density in acoustic metamaterials subjected to harmonic loading by one dimensional lattice representation. They found that effective mass density depends on frequency and becomes negative near resonant frequency of the internal mass by the classical elastic continuum approach. However, they mentioned that the dispersion of wave propagation and the band gap structure can be adequately described by microstructure continuum model. An experimental investigation of the

acoustic pressure in cavity of a two – dimensional sonic crystal has been conducted by Wu et al. [16]. They designed the sonic crystal with a two dimensional array of polymethyl methacrylate cylinders in air background. It was reported that for defective mode of the sonic crystal with a cavity, a full band gap was found near resonant frequency. Wu et al. [17] numerically calculated the band structure and obtained the defect band by using plane wave expansion and supercell calculation. They found the localized acoustic wave in defect zone. Espinosa, Jimenez and Torres [18] designed a structure made of an aluminum alloy plate with a square periodic arrangement of cylindrical holes filled with mercury. They tested the structure with ultrasonic transmission technique. At the frequency range between 1000 – 1120 kHz, there was no propagation of wave. Fang et al. [3] artificially designed ultrasonic Helmholtz resonator metamaterials with negative modulus. Their concept was based on flute mechanism. They calculated dispersion and transmission on the basis of homogenized media theory. A computational method to evaluate the material parameters of acoustic cloaks with arbitrary shape was proposed by Hu et al. [19]. They assumed harmonic transformation of the cloak layer which can be determined by Laplace's equation along with proper boundary conditions. Torrent and Sanchez – Dehesa [20] investigated that a wide range of isotropic acoustic metamaterials can be made by sonic crystal (SC) consisting of 2D arrangements of solid cylinders in a fluid or gas. By changing the

cylinders' diameters, a parabolic shape reflective index was achieved. Chen and Chan [21] mapped acoustic equation to Maxwell's equations of one polarization in the 2D geometry and to direct current conductivity equation in three dimensions in order to find out acoustic cloaking using coordinate transformation. Ambati et al. [22] reported that the surface excitations improve the transmission of evanescent pressure fields across the metamaterial. Zhang et al. [23] demonstrated experimentally the focusing of ultrasound waves with acoustic metamaterial network comprised of subwavelength Helmholtz resonators.

CHAPTER 3
THEORY

3.1 SOUND PROPAGATION IN STATIONARY CAVITY FLOW

Vibrating acoustic cavity where structure and fluid interface is predominant produces fluctuations in the pressure that are transferred through fluid media inside the cavity as elastic spring mechanism: a succession of compressions and rarefactions. The order of magnitude of acoustic pressure is usually small with respect to the undisturbed mean pressure. This conception infers to the linearization of the wave motion.

The compressions and rarefactions of fluid occur adiabatically in case of stationary fluid domain enclosed by structural domains. This approximation is good for low frequencies into audible frequency ranges from 20 Hz to 20 kHz. Since the wave lengths are longer at low frequency range, the viscous dissipation of fluid flow is weaker. The linear approximation of inviscid momentum equation is

$$\rho \frac{\partial^2 \overline{u}}{\partial t^2} + \nabla p = \overline{F_b} \tag{3.1}$$

It is permissible to interpret $\overline{F_b}$ as the localized force applied to the fluid domain at the interface of solid domain as structural acceleration which creates pressure to the fluid field.

The continuity equation of mass conservation,

$$\rho \frac{\partial \rho}{\partial t} + \frac{\partial}{\partial x}\left(\rho \dot{\overline{u}}\right) = 0 \tag{3.2}$$

Adiabatic bulk modulus of fluid is $B = \rho_0 \dfrac{\partial p}{\partial \rho}$ (3.3)

Therefore the continuity equation of mass conservation can be rewritten as $\frac{1}{c_s^2}\frac{\partial p}{\partial t} + \rho\frac{\partial \bar{\dot{u}}}{\partial x} = 0$ (3.4)

Taking the time derivative of continuity equation and the space derivative of momentum equation and substituting these equations, the classical wave equation can be rewritten as follow: $\frac{1}{c_s^2}\frac{\partial^2 p}{\partial t^2} = \frac{\partial^2 p}{\partial x^2}$ (3.5)

3.2 RAYLEIGH DAMPING

Damping plays a crucial role in dynamic structural analysis. However due to limitation of the exact mathematical co-relations of damping, the equivalent Rayleigh damping is the most effective way to incorporate damping parameters in the mathematical analysis of structures. Rayleigh damping is proportional to a linear combination effects of the stiffness and mass of the systems.

The generalized mathematical model of Rayleigh damping parameter in a three dimensional system is as follows:

$$\frac{\partial^2}{\partial t^2}\left(M\bar{U}\right) + \frac{\partial}{\partial t}\left(\xi C\bar{U}\right) + K\bar{U} = \overline{f(t)} \tag{3.6}$$

By space transformation and orthogonal properties of the system,

$$\bar{U} = \psi^T \bar{u}\psi \tag{3.7}$$

$$[M][\psi]^T\{\ddot{u}\}[\psi] + [\xi][\psi]^T\{\dot{u}\}[\psi] + [K][\psi]^T\{u\}[\psi] = [\psi]^T\{f(t)\} \tag{3.8}$$

The Rayleigh damping model is defined as the damping parameter C in terms of the mass M and the stiffness k as [C] = α [M] + β [K] in which

[C] = damping matrix of the physical system; [M] = mass matrix of the physical system; [K] = stiffness matrix of the system.

In order to find out the value of α and β, we need to know the damping ratio of the system at different natural frequencies by experiment.

$$\xi_i = \frac{1}{2}\left(\frac{\alpha}{2\pi \times f_i} + \beta \times 2\pi \times f_i\right) \tag{3.9}$$

Taking two natural frequencies and their respective damping ratios, two systems of equations of two unknown variables are formed. By solving these equations, we can find out α and β.

$$\begin{bmatrix} \frac{1}{4\pi \times f_1} & \pi \times f_1 \\ \frac{1}{4\pi \times f_2} & \pi \times f_2 \end{bmatrix} \begin{Bmatrix} \alpha \\ \beta \end{Bmatrix} = \begin{bmatrix} \xi_1 \\ \xi_2 \end{bmatrix} \tag{3.10}$$

In the practical engineering analysis, the design engineers presume a constant damping ratio for the overall system based on their experience and standard literature review. In fact, the mass participation is prominent at first few natural frequencies and then decreases at higher modes. The mass participation can be inferred by $\omega = \sqrt{K/M}$. Considering critical damping, $C_c = 2\sqrt{KM}$, it can be concluded that for successive modes with reduction in modal mass, Cc will decrease with increase in mode.

CHAPTER 4
PHYSICAL MODEL

The physical model considered here is shown in Fig. 4.1, along with the important geometric parameters. It consists of a rectangular cavity filled with air. An array of wire stems with mass of copper attached at the top of each stem, have been connected at the base of the structural cavity. The size of the rectangular cavity is 152.4 mm x 12.7 mm x 38.1 mm with thickness of 1.5875 mm on all sides of the cavity whereas the base of the structure is 6.35 mm thick. The rectangular acoustic cavity is made of PMMA (polymethyl methacrylate). The copper masses are covered with epoxy resin and aliphatic polyaminel polyamide hardener to make the copper mass well mounted with the wire stems.

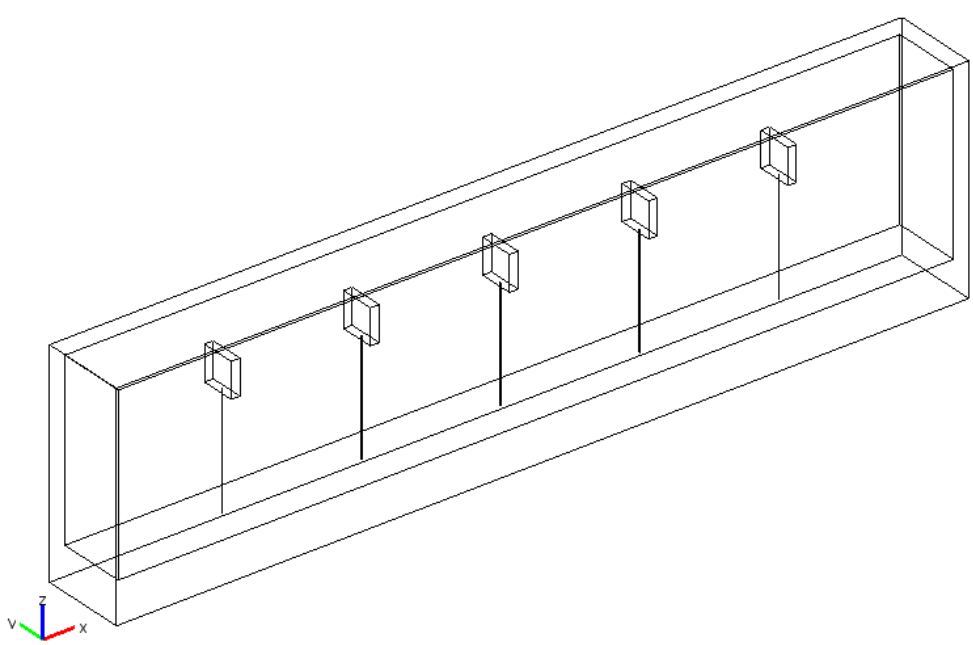

Fig 4.1: physical model

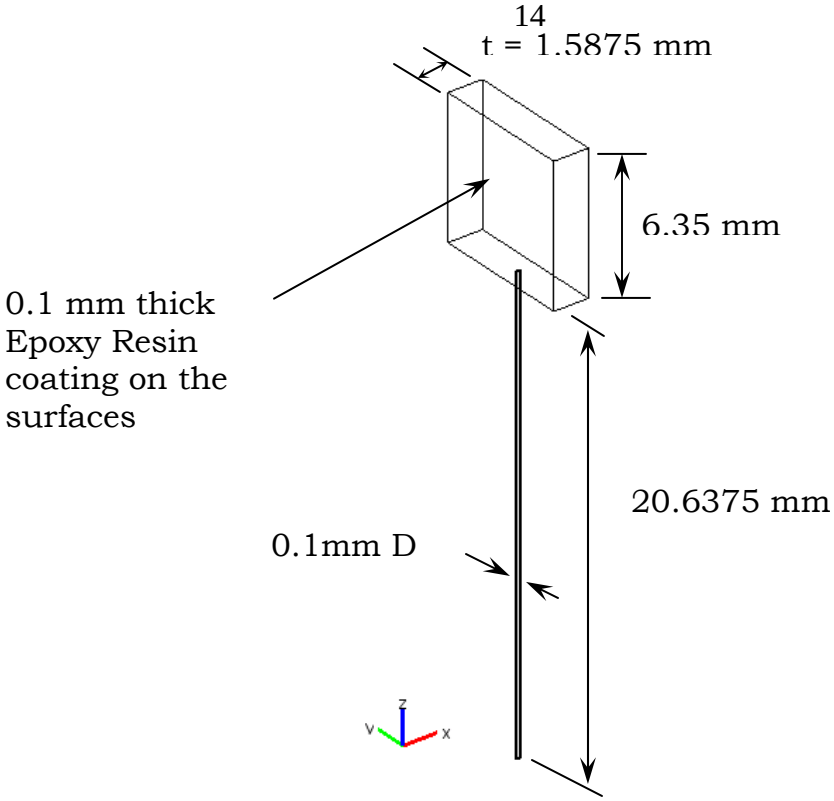
t = 1.5875 mm
6.35 mm
0.1 mm thick
Epoxy Resin
coating on the
surfaces
20.6375 mm
0.1mm D

(a)

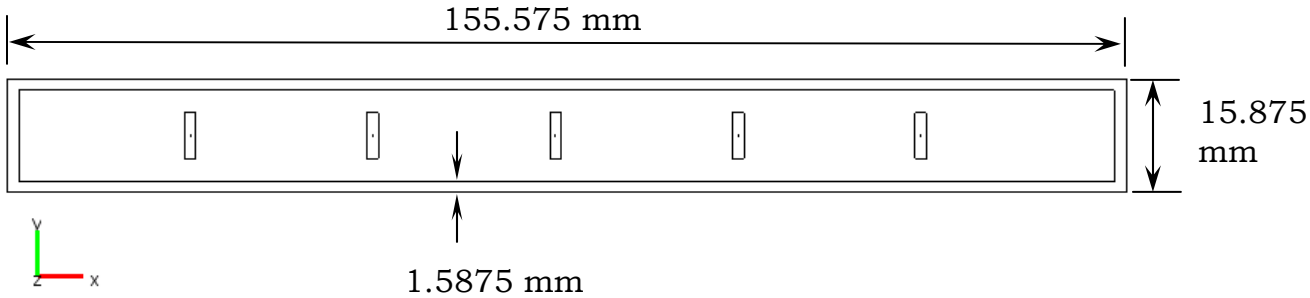
155.575 mm
15.875
mm
1.5875 mm

(b)

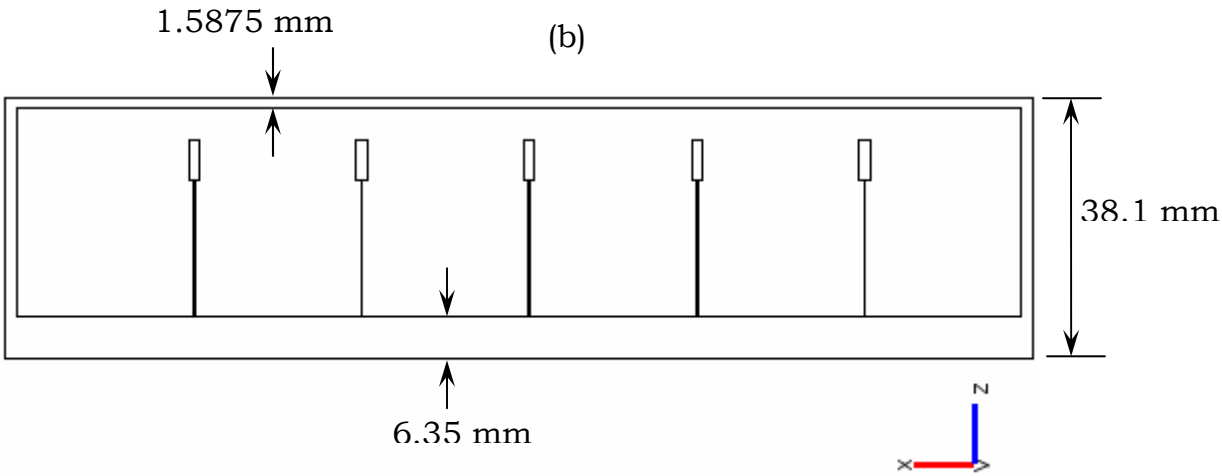
1.5875 mm
38.1 mm
6.35 mm

(c)

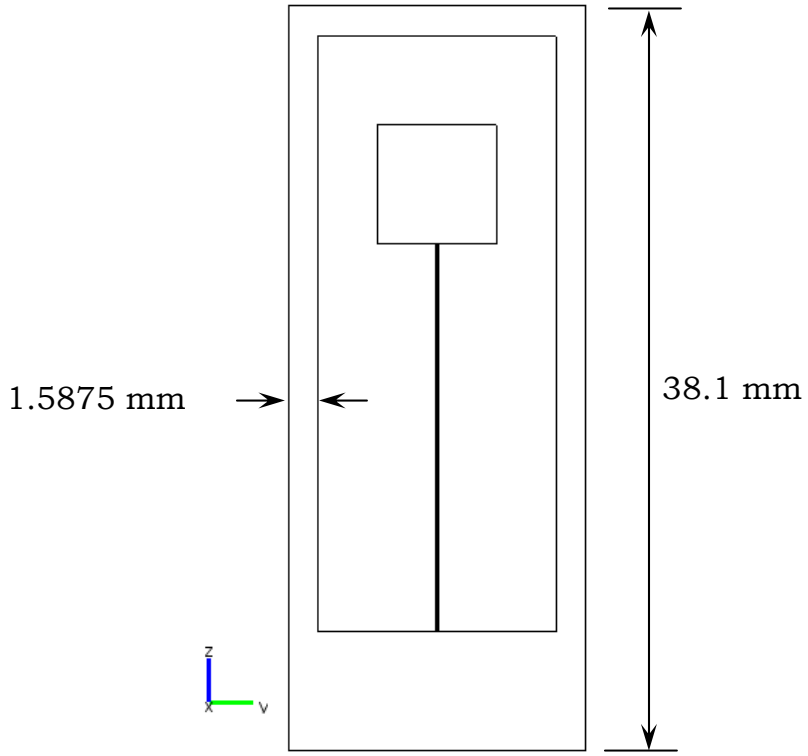

Fig. 4.2: design parameters of the vibro-acoustic metamaterial

The design parameters of the vibro-acoustic metamaterial have been reported in fig. 4.2. The shape memory alloy has been chosen for fabricating stems due to its flexibility towards motions. The five stems have been implanted in such a way that the minimum gap between two stems must meet the maximum deflection or bending criterion without direct physical contact among each other. The material specification has been represented in table 4.1.

Table 4.1: Material Properties of the complex structure

PMMA [24]	
Young's Modulus, E (GPa)	$3x10^9$
Poisson ratio, ν	0.4
Density, ρ (kg/m^3)	1190
SHAPE MEMORY ALLOY [24]	
Young's Modulus, E (GPa)	$75x10^9$
Poisson ratio, ν	0.3
Density, ρ (kg/m^3)	6450
COPPER	
Young's Modulus, E (GPa)	$110x10^9$
Poisson ratio, ν	0.35
Density, ρ (kg/m^3)	8700
EPOXY RESIN	
Young's Modulus, E (GPa)	$110x10^9$
Poisson ratio, ν	0.343
Density, ρ (kg/m^3)	2600
AIR AT 20°C TEMP	
Density, ρ (kg/m^3)	1.25
Speed of sound (m/s)	343

CHAPTER 5
EXPERIMENTAL ANALYSIS

5.1 EXPERIMENTAL SETUP

In the present experiment as shown in figure 5.1, a rectangular acoustic cavity with square masses mounted on an array of stems attached at the base of the cavity has been tested experimentally. The hammer has hard tip (50 lbf pk). Its sensitivity is 100 mV/lbf. The frequency analyzer used here has a wide range from 0 to 20 kHz. The analyzer samples the data from the experiment and sends them to the computer based data acquisition software. The software has the capability to plot time domain and frequency domain graphs simultaneously.

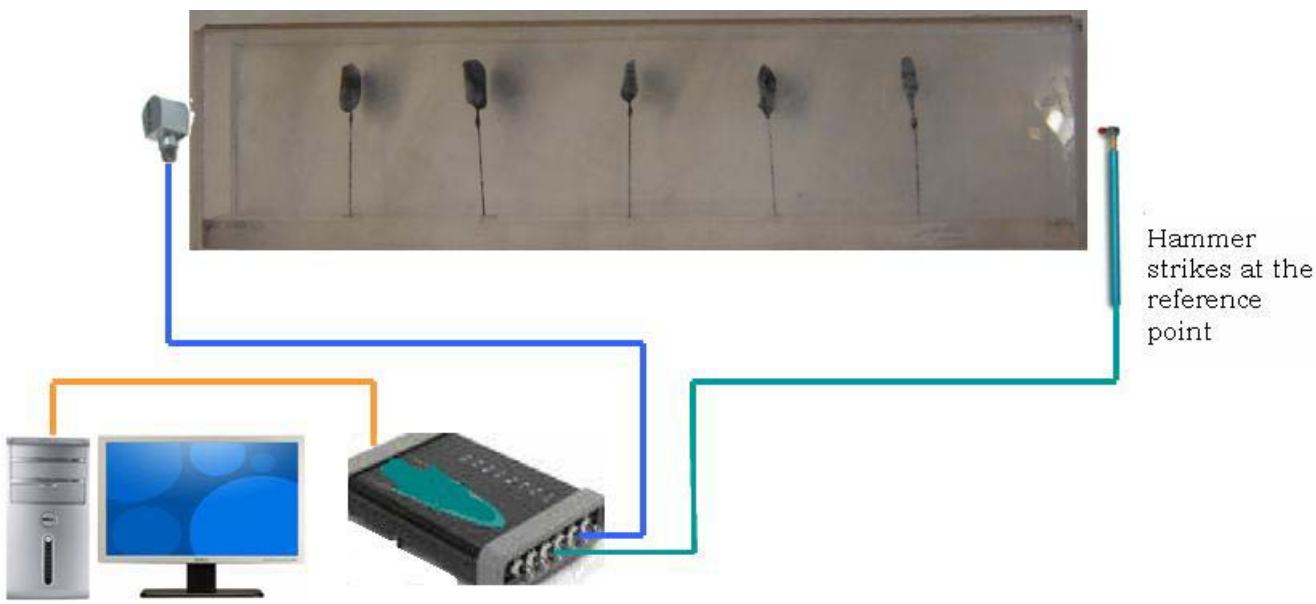

Fig. 5.1: Schematic diagram of experimental setup

During the test, averaging of three separate strikes has been taken for good results. The hamming window has been selected and the resolution of the data acquisition is 400.

5.2 EXPERIMENTAL RESULTS

Since the designed object is complex structure, it has a number of different natural frequencies within the range from 0 Hz to 20 kHz. The natural frequencies of a system can be determined by the peak values of the magnitude of the transfer function or by observing the 90 degree phase shift [25]. If the damping ratio of a system is high, the natural frequencies can not be estimated by only observing the peak values of transfer function magnitude plot. At the damping scenario, the 90 degree phase shift has to be considered simultaneously [25]. The conducted experimental test infers that the complex system, subjected to 0.58 g external impulse forcing as shown in fig. 5.2 (b), has underdamped attribution. Figure 5.2 (a) demonstrates that the system has dissipated kinetic energy per half of the unit mass, $K.E. \alpha V^2$, gradually at each overshoot in order to reach in stable static condition. The order of magnitude of the kinetic energy per half of unit mass is reduced at approximately 5 msec.

The damping ratios of the complex system at different natural frequencies have been calculated by taking half – power points of the response curve of the system. Therefore, the magnitude of the transfer function has been plotted in decibel. The damping ratios at different

natural frequencies have been measured by taking two frequencies at 6 dB down from the peak response for acceleration dB.

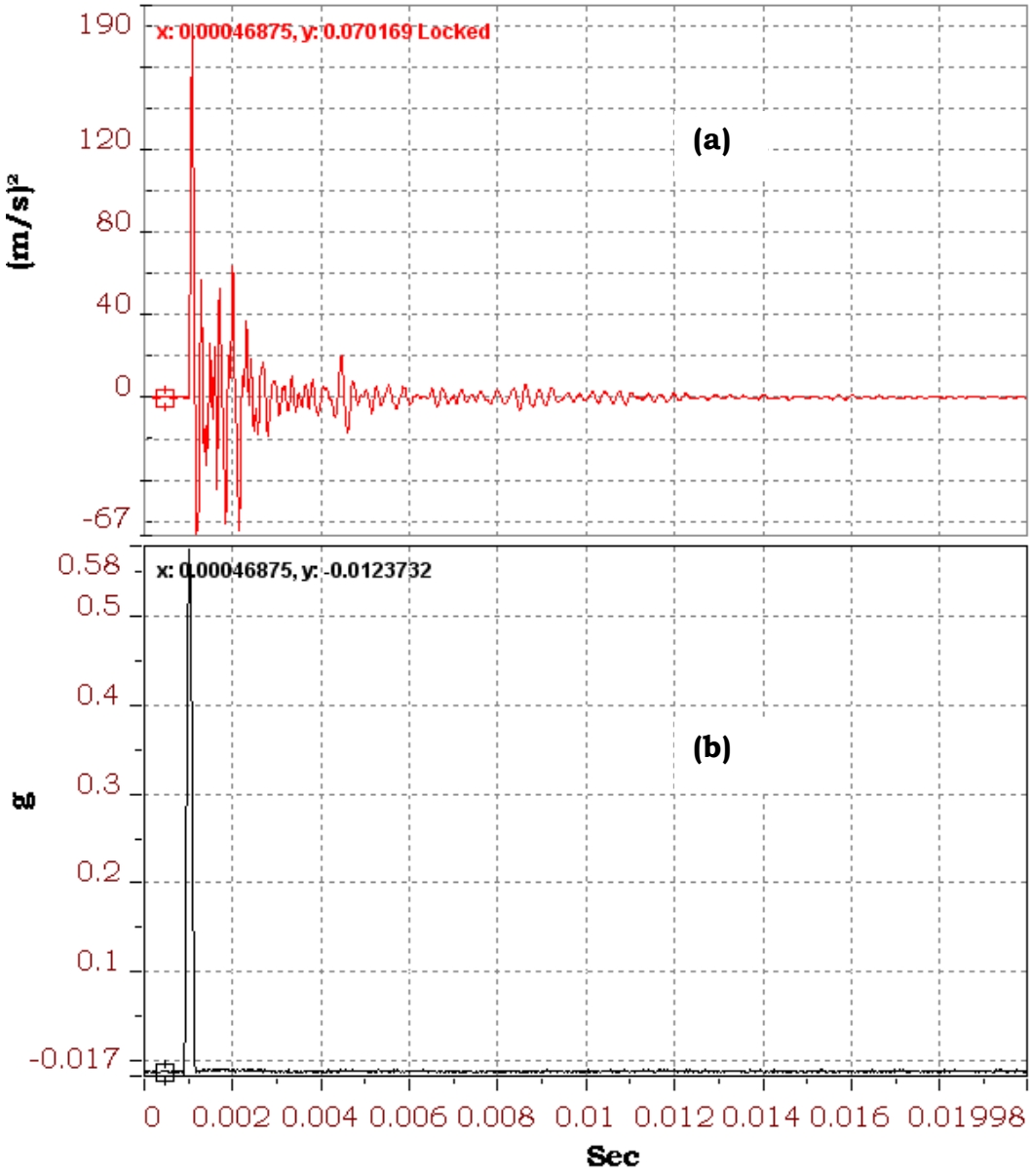

Fig. 5.3: transient response of acoustic metamaterial (a) square of velocity profile (b) impulse force

Figure 5.3 (a), and (b) show the phase shift and magnitude plot of transfer function of motion versus impulse loading. The accuracy of the test has been confirmed by observing the fig. 5.3 (c) in which there is no

significant fluctuation of line spectrum of input impulse force. If there are double strikes at each tapping by hammer, the curve will fluctuate.

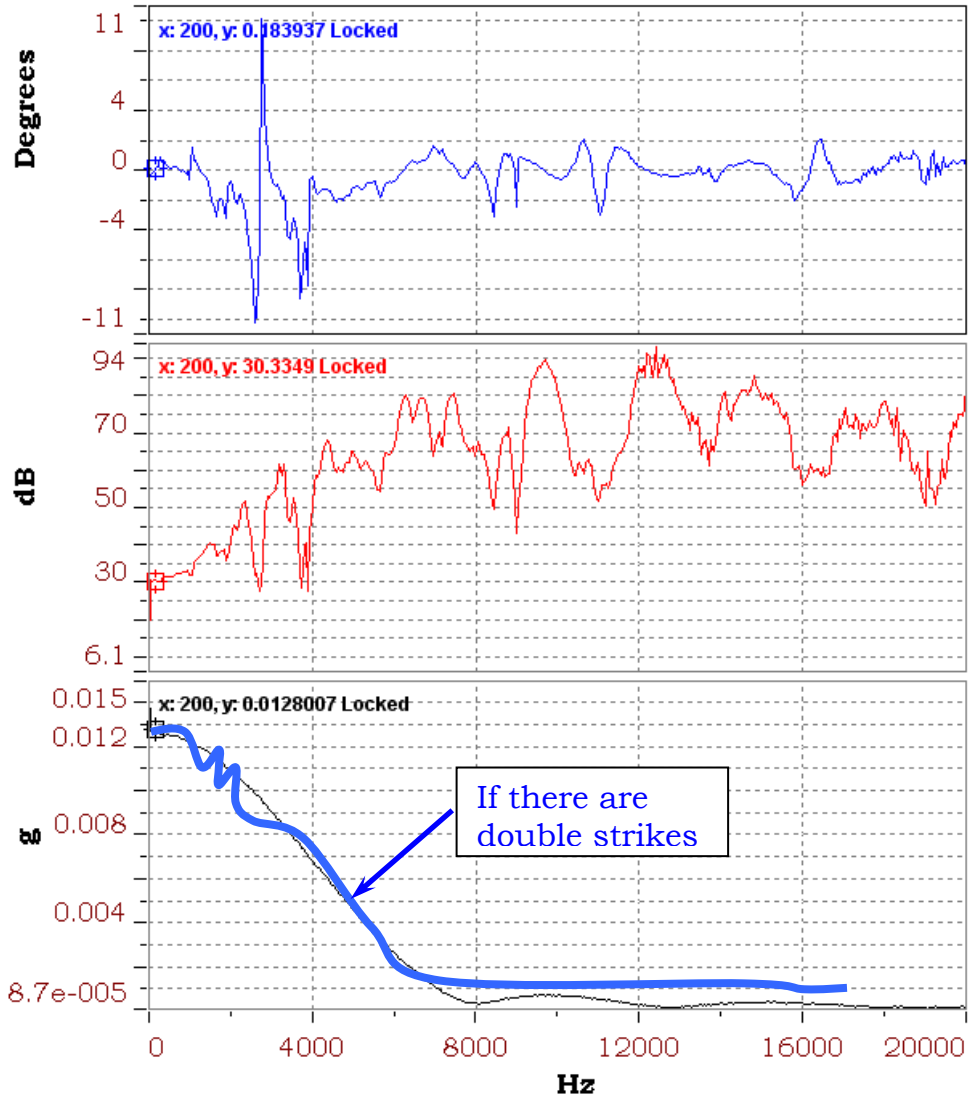

Fig. 5.3: (a) magnitude plot of transfer function (b) phase plot of transfer function and (c) line spectrum of impulse force

5.2.3 EVALUATION OF RAYLEIGH DAMPING PARAMETERS

Figure 5.4 represents the damping ratios of the complex system at different natural frequencies. After best fitting the experimental data, it

shows that the damping ratio decreases exponentially with respect to natural frequencies. By taking the damping ratios at two natural frequencies, the Rayleigh damping parameters for mass participation in damping and stiffness dominant damping have been calculated by using equation 3.10.

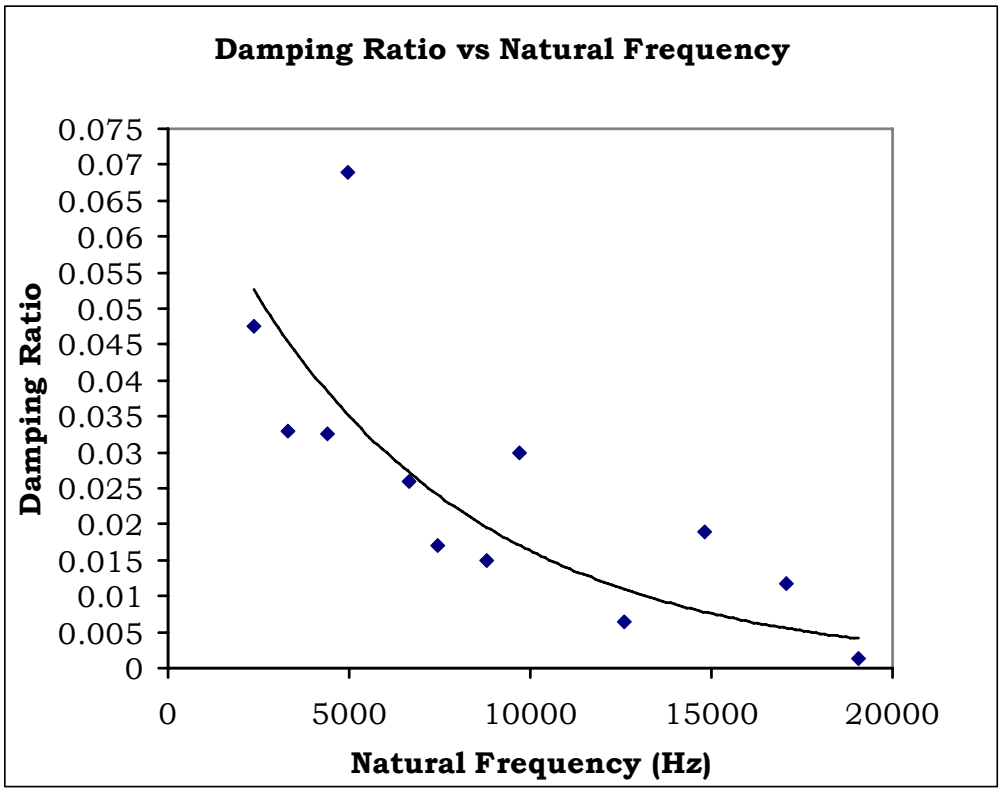

Fig. 5.4: variation of damping ratio with natural frequency

The value of mass damping parameter is 1489.84 (1/sec) while that of stiffness damping parameter is 1.319×10^{-7} (sec). Therefore, it can be conjectured that the contribution of the mass of the designed complex system in damping is significantly higher than the stiffness of the system.

Milton and Willis [6] proposed the modification of Newton's second law of motion and linear continuum elastodynamics. They developed mathematical model to introduce the negative effective mass effect in a series of mass – in – mass configuration. It is mentioned that the natural behavior of their complex structure follows the motion of large mass. However, Huang et al. [4] proposed a mathematical model considering the influence of localized resonance frequencies of the internal masses in calculating the effective mass of the complex structure. In the present study, we have proposed the combined effect of large mass and the internal masses. Since the motion of large mass and internal masses is relativistic, the effective mass of internal masses itself depends on the natural behavior of large mass.

Therefore,

$$M_{eff} = f(M_1,\ m \in f(\omega_{0,structure}))$$
$$= M_1 + \frac{m\omega_0^2}{\omega_0^2 - \omega^2}$$

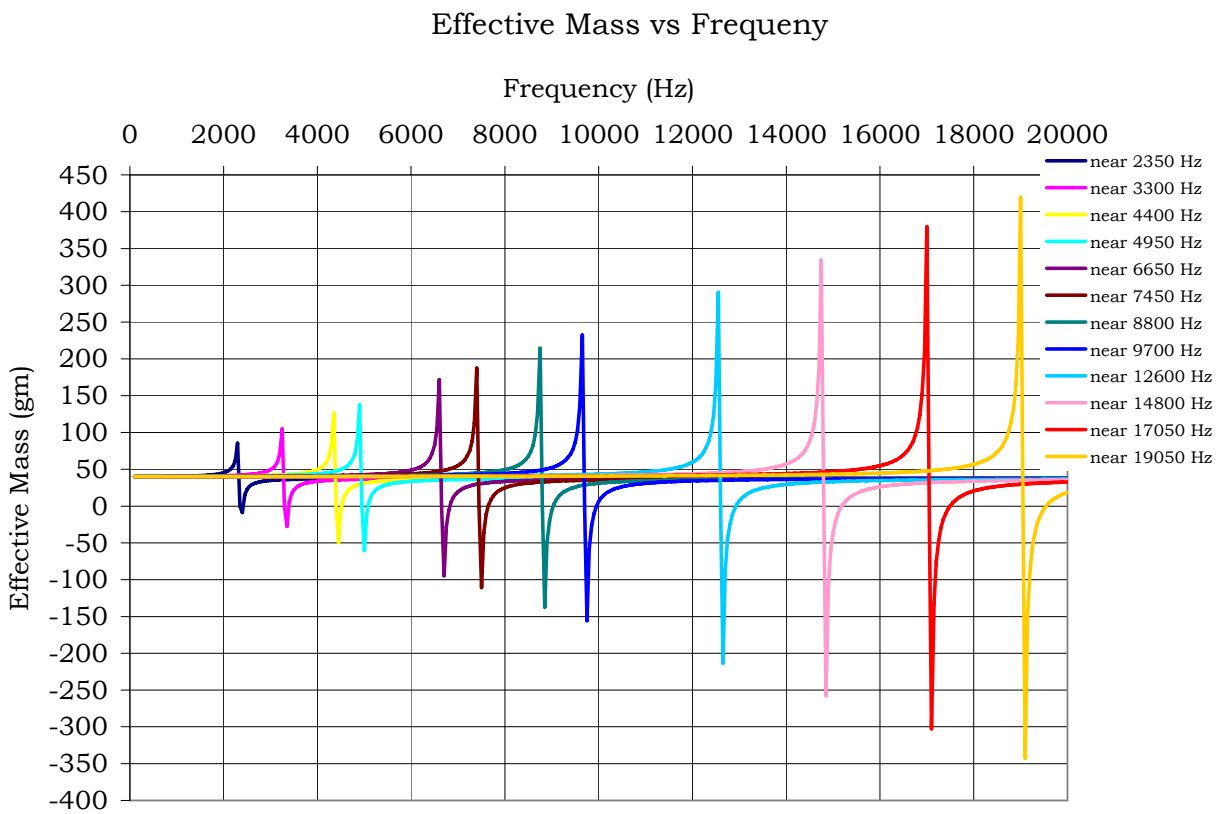

Fig. 5.5: Asymptotic nature of effective mass near natural frequencies

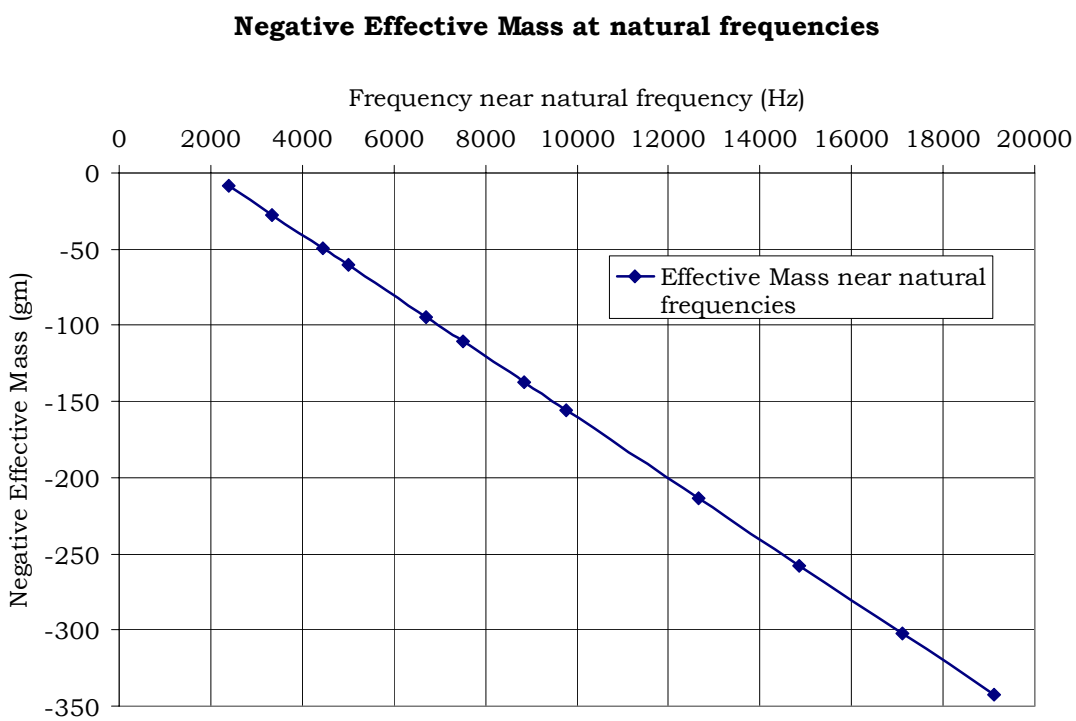

Fig. 5.6: influence of higher order natural frequencies on effective mass

CHAPTER 6
MATHEMATICAL MODELING

6.1 GOVERNING EQUATIONS

Vibro – acoustic metamaterial has been designed on the concept of multiphysics phenomenon where the pressure of the fluid inside the cavity creates fluid load on the solid domain at acoustic – structure interface and the acceleration of the structures affect the fluid domain as a normal acceleration on the interface.

Assumptions:

1) small displacements in solid
2) composite of isotropic materials
3) cavity is filled by incompressible, inviscid fluid (air)

Structural Mechanics:

$$\varepsilon_x = \frac{\partial u}{\partial x} \qquad \varepsilon_y = \frac{\partial v}{\partial y} \qquad \varepsilon_z = \frac{\partial w}{\partial z}$$
$$\varepsilon_{xy} = \frac{1}{2}\left(\frac{\partial u}{\partial y} + \frac{\partial v}{\partial x}\right) \quad \varepsilon_{yz} = \frac{1}{2}\left(\frac{\partial v}{\partial z} + \frac{\partial w}{\partial y}\right) \quad \varepsilon_{zx} = \frac{1}{2}\left(\frac{\partial u}{\partial z} + \frac{\partial w}{\partial x}\right) \tag{6.1}$$

The symmetric strain tensor comprises of both normal and shear strain components:

$$\varepsilon = \begin{bmatrix} \varepsilon_x & \varepsilon_{xy} & \varepsilon_{xz} \\ \varepsilon_{xy} & \varepsilon_y & \varepsilon_{yz} \\ \varepsilon_{xz} & \varepsilon_{yz} & \varepsilon_z \end{bmatrix} \tag{6.2}$$

The symmetric stress tensor describes stress in a material:

$$\sigma = \begin{bmatrix} \sigma_x & \tau_{xy} & \tau_{xz} \\ \tau_{yx} & \sigma_y & \tau_{yz} \\ \tau_{zx} & \tau_{zy} & \sigma_z \end{bmatrix} \quad \tau_{xy} = \tau_{yz} \quad \tau_{xz} = \tau_{zx} \quad \tau_{yz} = \tau_{zy} \tag{6.3}$$

The constitutive equation $\sigma = D\varepsilon$

$$D^{-1} = \frac{1}{E}\begin{bmatrix} 1 & -\nu & -\nu & 0 & 0 & 0 \\ -\nu & 1 & -\nu & 0 & 0 & 0 \\ -\nu & -\nu & 1 & 0 & 0 & 0 \\ 0 & 0 & 0 & 2(1+\nu) & 0 & 0 \\ 0 & 0 & 0 & 0 & 2(1+\nu) & 0 \\ 0 & 0 & 0 & 0 & 0 & 2(1+\nu) \end{bmatrix} \tag{6.4}$$

Physics of Acoustics:

Sound waves in a lossless medium are governed by the following equation for acoustic pressure $p(x,y,z,t) = p(x,y,z,t)e^{i\omega t}$

$$\nabla \cdot \left(-\frac{1}{\rho_o}\left(\nabla p - \bar{q}\right)\right) - \frac{\omega^2 p}{\rho_o c_s^2} = Q \tag{6.5}$$

$$\nabla \cdot \left(-\frac{1}{\rho_o}\left(\nabla p\right)\right) = \frac{\omega^2 p}{\rho_o c_s^2} \tag{6.6}$$

6.2 BOUNDARY CONDITIONS

Coupling of structure and acoustic physics at interfaces:

$$\bar{n} \cdot \left(\frac{1}{\rho_o}\left(\nabla p\right)\right) = -a_n \tag{6.7}$$

where a_n is external source term and $\bar{n}$ is inward normal direction of acceleration.

Structural acceleration: $a_n = \bar{n} \cdot \overline{u_{tt}}$ (6.8)

Fluid loading: $\overline{F}_p = -\overline{n}_s p$ (6.9)

The physical model has been subjected to unit loading (1N). The outer boundaries of the solid structure have been kept free of constraints whereas the inner boundaries of the solid structure have been coupled due to solid - acoustic interface.

CHAPTER 7
COMPUTATIONAL DETAILS

7.1 GENERAL

The wave theory of sound comprises of continuum physics: the conservation of mass and Eulerian motion of fluid as pressure pulse transferring through its neighboring particles, which correlates pressure and density of matters. However, sound wave is generated by the perturbation of ambient state which results from some external applied forces or the vibration of structures. Acoustic cavity enclosed by solid domain is considered here for computational interpretation. To visualize the solid – acoustics interaction inside the acoustic cavity, an approximate numerical solution is required which can be obtained by CFD code. The partial differential equations of acoustics wave equation and solid mechanics are discretized in order to obtain a system of approximate algebraic equations, which then can be solved on a computer. The approximations are applied to small domains in space and/ or time so the numerical solution provides results at discrete locations in space and time. Much as accuracy of experimental data depends on the quality of the tools used, the accuracy of numerical solution is dependent on the quality of discretization used.

CFD computation involves the creation of a set numbers that constitutes a realistic approximation of a real life system. The outcome of computation process improves the understanding of the behavior of a

system. Thereby, engineers need CFD codes that can produce physically realistic results with good accuracy in simulations with finite grids. Contained within the broad field of computational fluid dynamics are activities that cover the range from the automation of well established engineering design methods to the use of detailed solutions of the acoustics wave equation coupled with structural mechanics as substitutes for experimental research into the nature of complex flows and multi-physics interferences. It is more frequently used in fields of engineering where the geometry is complicated or some important feature that cannot be dealt with standard methods.

The conservation of mass, the acoustics wave equation, solid mechanics and the coupled structure – acoustics interface are considered to be the correct mathematical description of the governing equations of structural vibration and consequent sound propagation.

There are several discritization methods available for the high performance numerical computation in CFD.

- Finite volume method (FVM)
- Finite element method (FEM)
- Finite difference method (FDM)
- Boundary element method (BEM)
- Boundary volume method (BVM)

In the present numerical computation, galerkin finite element method (FEM) is used.

7.2 FINITE ELEMENT METHOD

The finite element method (FEM) is a powerful computational technique for solving problems which are described by partial differential equations or can be formulated as functional minimization. The basic idea of the finite element method is to view a given domain as an assemblage of simple geometric shapes, called finite elements, for which it is possible to systematically generate the approximation functions needed in the solution of partial differential equations by the variational or weighted residual method. The computational domains with irregular geometries by a collection of finite elements makes the method a valuable practical tool for the solution of boundary, initial and eigen value problems arising in various fields of engineering. The approximation functions, which satisfy the governing equations and boundary conditions, are often constructed using ideas from interpolation theory. Approximating functions in finite elements are determined in terms of nodal values of a physical field which is sought. A continuous physical problem is transformed into a discretized finite element problem with unknown nodal values. For a linear problem, a system of linear algebraic equations should be solved. Values inside finite elements can be recovered using nodal values.

The major steps involved in finite element analysis of a typical problem are:

1. Discretization of the domain into a set of finite elements (mesh generation).
2. Weighted-integral or weak formulation of the differential equation to be analyzed.
3. Development of the finite element model of the problem using its weighted-integral or weak form.
4. Assembly of finite elements to obtain the global system of algebraic equations.
5. Imposition of boundary conditions.
6. Solution of equations.
7. Post-computation of solution and quantities of interest.

7.3 MESH GENERATION

In finite element method, the mesh generation is the technique to subdivide a domain into a set of subdomains, called finite elements. Figure shows a domain, Ω is subdivided into a set of subdomains, Ω^e with boundary Γ^e.

The present numerical technique will discretize the computational domain into unstructured triangles by Delaunay Triangular method. The Delaunay triangulation is a geometric structure that has enjoyed great popularity in mesh generation since the mesh generation was in its infancy. In two dimensions, the Delaunay triangulation of a vertex set maximizes the minimum angle among all possible triangulations of that vertex set.

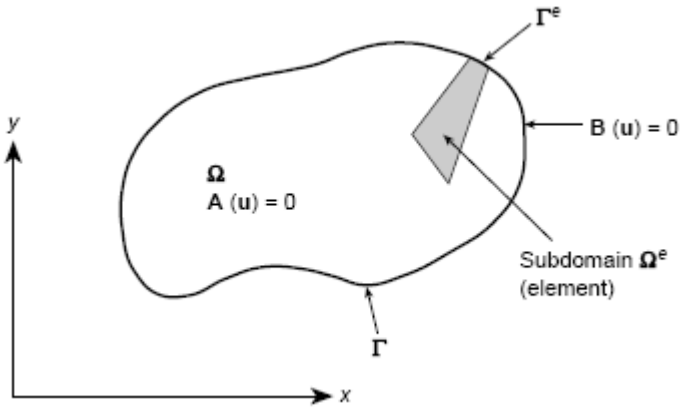

Figure 7.1: Finite element discretization of a domain

Figure 7.2 shows the mesh mode for the present numerical computation. Mesh generation has been done meticulously. Tetrahedral elements with advance triangular form have been considered to void the inverted elements.

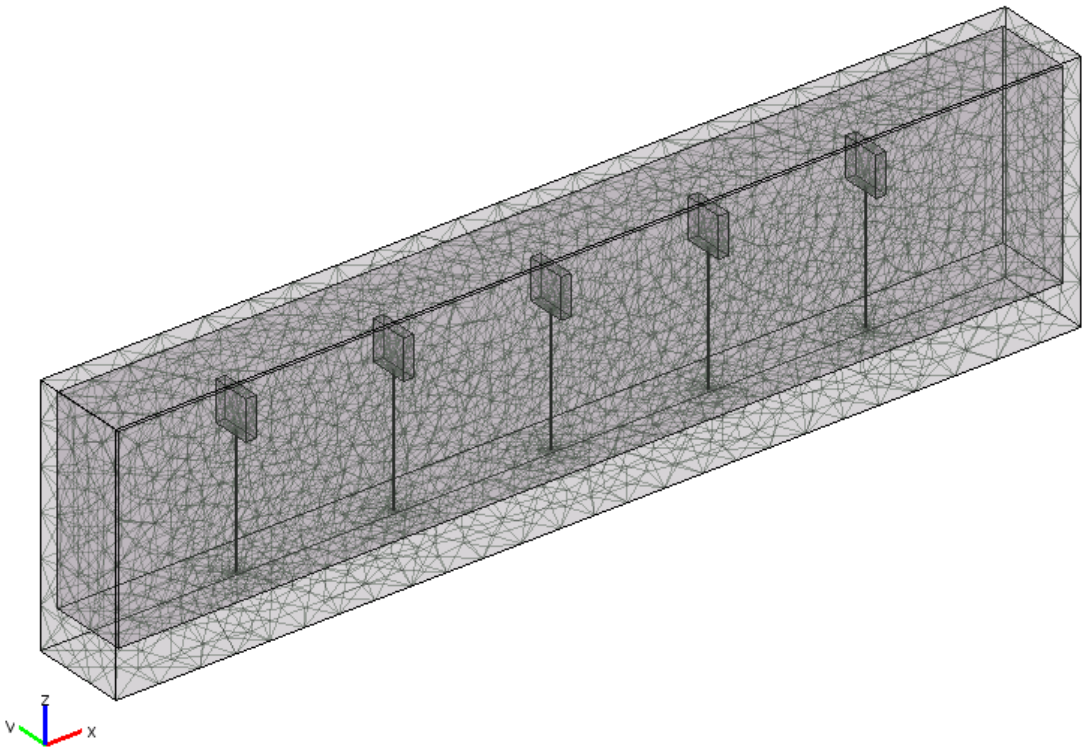

Fig. 7.2: Current mesh structure with 231843 numbers of nodes for acoustic cavity problem

7.4 CONVERGENCE TEST

Figure 7.3 shows the convergence test of acoustic metamaterial at 500 Hz excitation frequency. The frequency response analysis of metamaterial depicts that the amplitude of the displacement at the target probe point becomes invariant after 231843 degree of freedoms. For the optimization of computational cost and the accuracy of the results, 231843 degree of freedoms has been chosen.

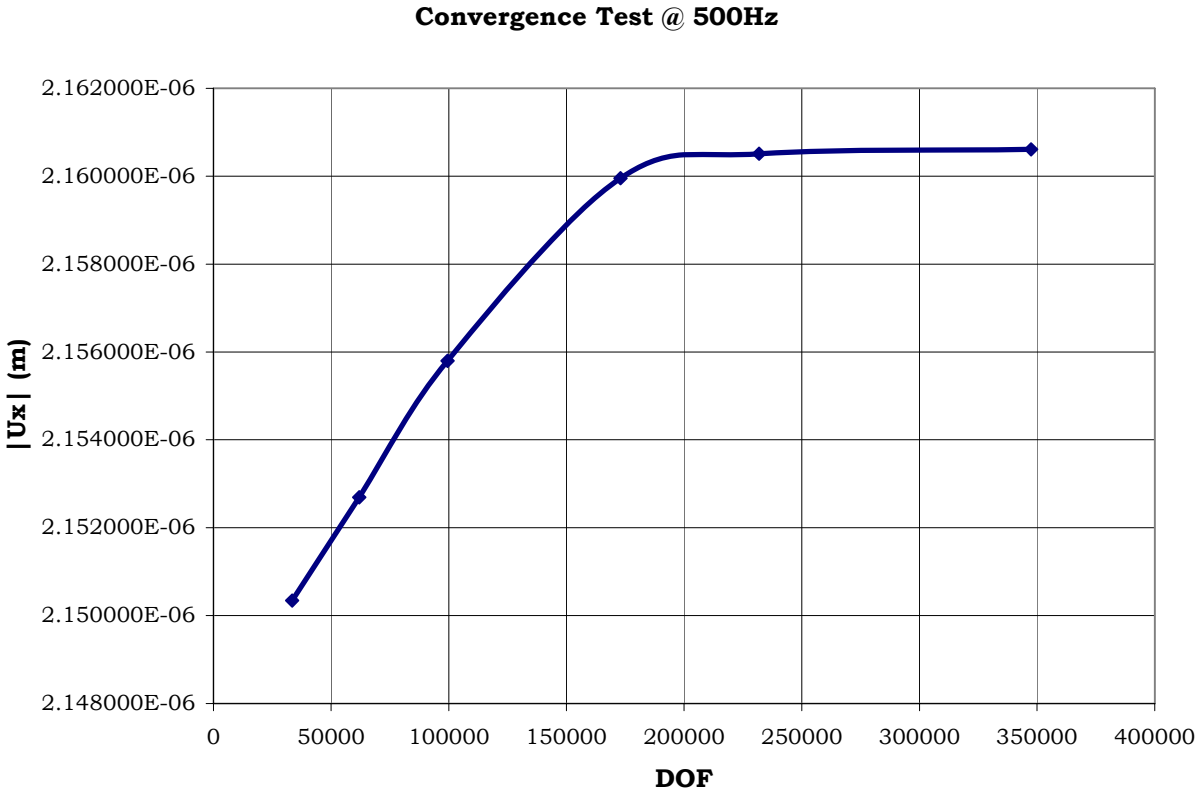

Fig. 7.3: convergence test of acoustic metamaterial at 500 Hz time harmonic excitation frequency

7.5 ALGORITHM

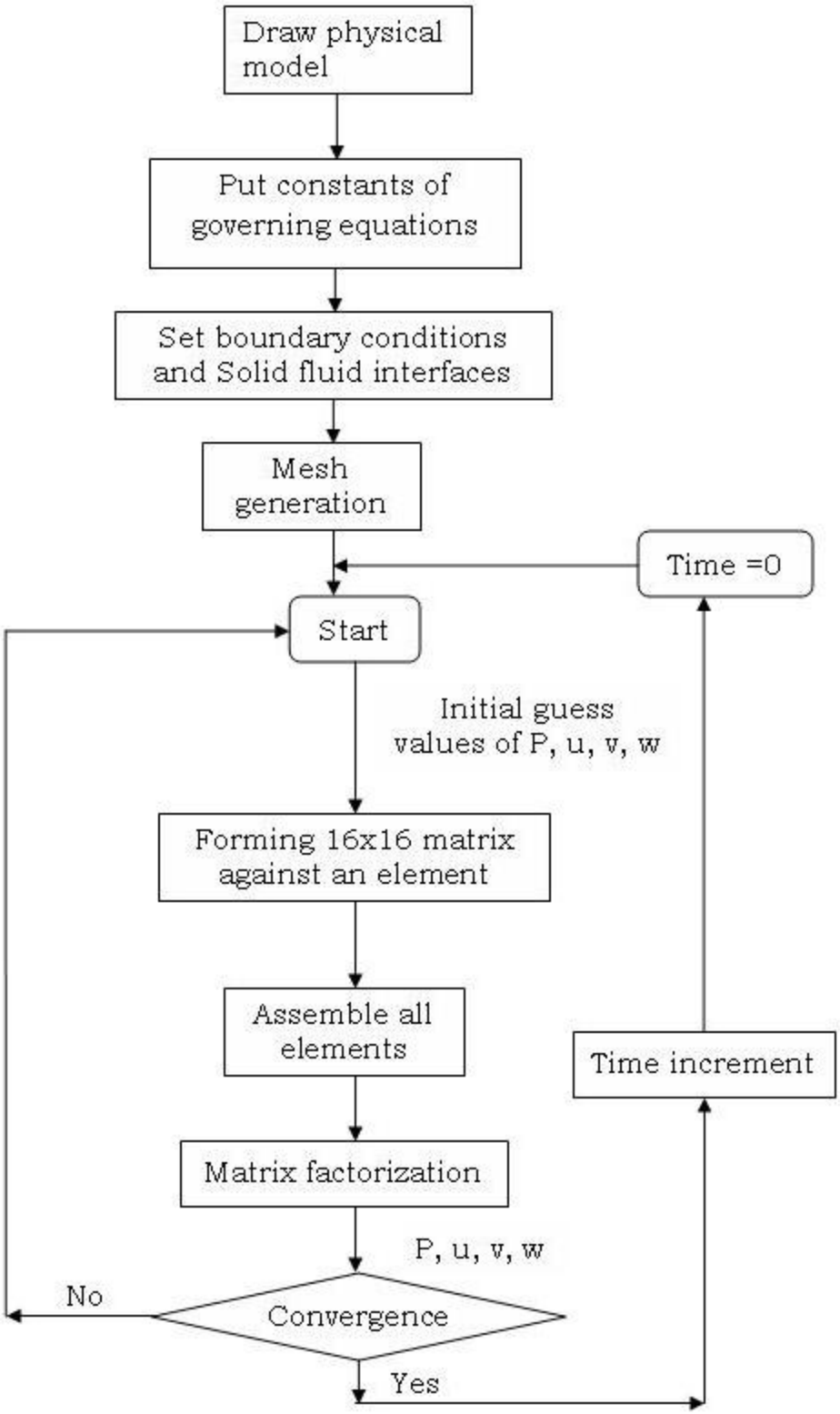

In the iterative Newton-Raphson algorithm, the discrete forms of the continuity, acoustics wave equation and stress – strain equation are solved to find out the value of the surface plot of acoustic pressure's magnitude and phase and the deformed shape of the solid domains. It is essential to guess the initial values of the variables. Then the numerical solutions of the variables are obtained while the convergent criterion $|u,v,w,p|_{t+\Delta t} - |u,v,w,p|_t \leq 10^{-6}$ is fulfilled.

7.6 SOLUTIONS OF SYSTEMS OF EQUATIONS

A system of linear algebraic equations has been solved by the UMFPACK of COMSOL Multiphysics [26] with MATLAB interface. UMFPACK is a set of routines for solving unsymmetric sparse linear systems, **Ax** = **b**, using the Unsymmetric MultiFrontal method and direct sparse LU factorization. Five primary UMFPACK routines are required to factorize **A** or **Ax** = **b**:

1. Pre-orders the columns of A to reduce fill-in and performs a symbolic analysis.
2. Numerically scales and then factorizes a sparse matrix.
3. Solves a sparse linear system using the numeric factorization.
4. Frees the Symbolic object.
5. Frees the Numeric object.

Additional routines are:

1. Passing a different column ordering
2. Changing default parameters

3. Manipulating sparse matrices
4. Getting **LU** factors
5. Solving the **LU** factors
6. Computing determinant

UMFPACK factorizes **PAQ**, **PRAQ**, or $\mathbf{PR^{-1}AQ}$ into the product **LU**, where **L** and **U** are lower and upper triangular, respectively, **P** and **Q** are permutation matrices, and **R** is a diagonal matrix of row scaling factors (or **R** = **I** if row-scaling is not used). Both **P** and **Q** are chosen to reduce fill-in (new nonzeros in **L** and **U** that are not present in **A**). The permutation **P** has the dual role of reducing fill-in and maintaining numerical accuracy (via relaxed partial pivoting and row interchanges). The sparse matrix **A** can be square or rectangular, singular or non-singular, and real or complex (or any combination). Only square matrices **A** can be used to solve **Ax** = **b** or related systems. Rectangular matrices can only be factorized. UMFPACK first finds a column pre-ordering that reduces fill-in, without regard to numerical values. It scales and analyzes the matrix, and then automatically selects one of three strategies for pre-ordering the rows and columns: unsymmetric, 2-by-2, and symmetric. These strategies are described below.

The column pre-ordering of S is computed by COLAMD. The method finds a symmetric permutation Q of the matrix STS (without forming STS explicitly). This is a good choice for Q, since the Cholesky factors of (SQ)T(SQ) are an upper bound (in terms of nonzero pattern) of the factor

U for the unsymmetric LU factorization (PSQ = LU) regardless of the choice of P [19, 20, 22]. This modified version of COLAMD also computes the column elimination tree and post-orders the tree. It finds the upper bound on the number of nonzeros in L and U. It also has a different threshold for determining dense rows and columns. During factorization, the column pre-ordering can be modified. Columns within a single super-column can be reshuffled, to reduce fill-in. Threshold partial pivoting is used with no preference given to the diagonal entry. Within a given pivot column j, an entry a_{ij} can be chosen if $|a_{ij}| \geq 0.1 \max |a_{*j}|$. Among those numerically acceptable entries, the sparsest row i is chosen as the pivot row.

One notable attribute of the UMFPACK is that whenever a matrix is factored, the factorization is stored as a part of the original matrix so that further operations on the matrix can reuse this factorization. Whenever a factorization or decomposition is calculated, it is preserved as a list (element) in the factor slot of the original object. In this way a sequence of operations, such as determining the condition number of a matrix and then solving a linear system based on the matrix, do not require multiple factorizations of the intermediate results.

Conceptually, the simplest representation of a sparse matrix is as a triplet of an integer vector **i** giving the row numbers, an integer vector **j** giving the column numbers, and a numeric vector **x** giving the non-zero values in the matrix. The triplet representation is row-oriented if

elements in the same row were adjacent and column-oriented if elements in the same column were adjacent. The compressed sparse row (csr) or compressed sparse column (csc) representation is similar to row-oriented triplet or column-oriented triplet respectively. These compressed representations remove the redundant row or column in indices and provide faster access to a given location in the matrix.

CHAPTER 8
RESULTS AND DISCUSSION

The numerical results presented here are based on time harmonic analysis. The physical model has been excited by unit loading over a frequency range from 0 to 20 kHz. Figure 8.1 shows the frequency response of the complex structure. The natural frequencies of the complex designed model obtained by numerical analysis have close agreement with the experimentally obtained natural frequencies as shown in table 8.1. The first peak has been rescinded due to rigid body motion.

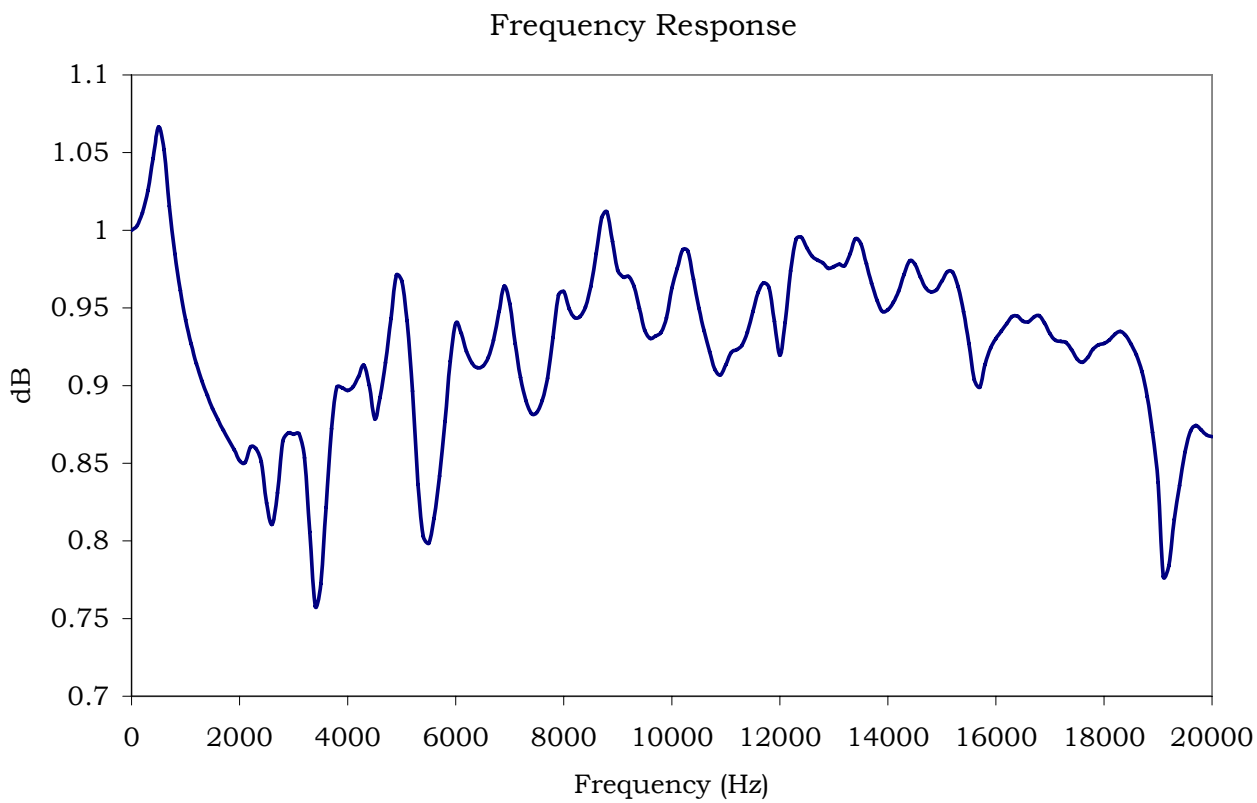

Fig. 8.1: Frequency response of the complex structure

Table 8.1: Close agreement between experiment and computation

Experimental Natural Frequencies (Hz)	**Numerical Natural Frequencies (Hz)**
2350	2300
3300	2900
4400	4300
4950	4900
6650	6900
7450	8000
8800	8800
9700	10300
12400	12600
14500	14800
16800	17050
19700	19050

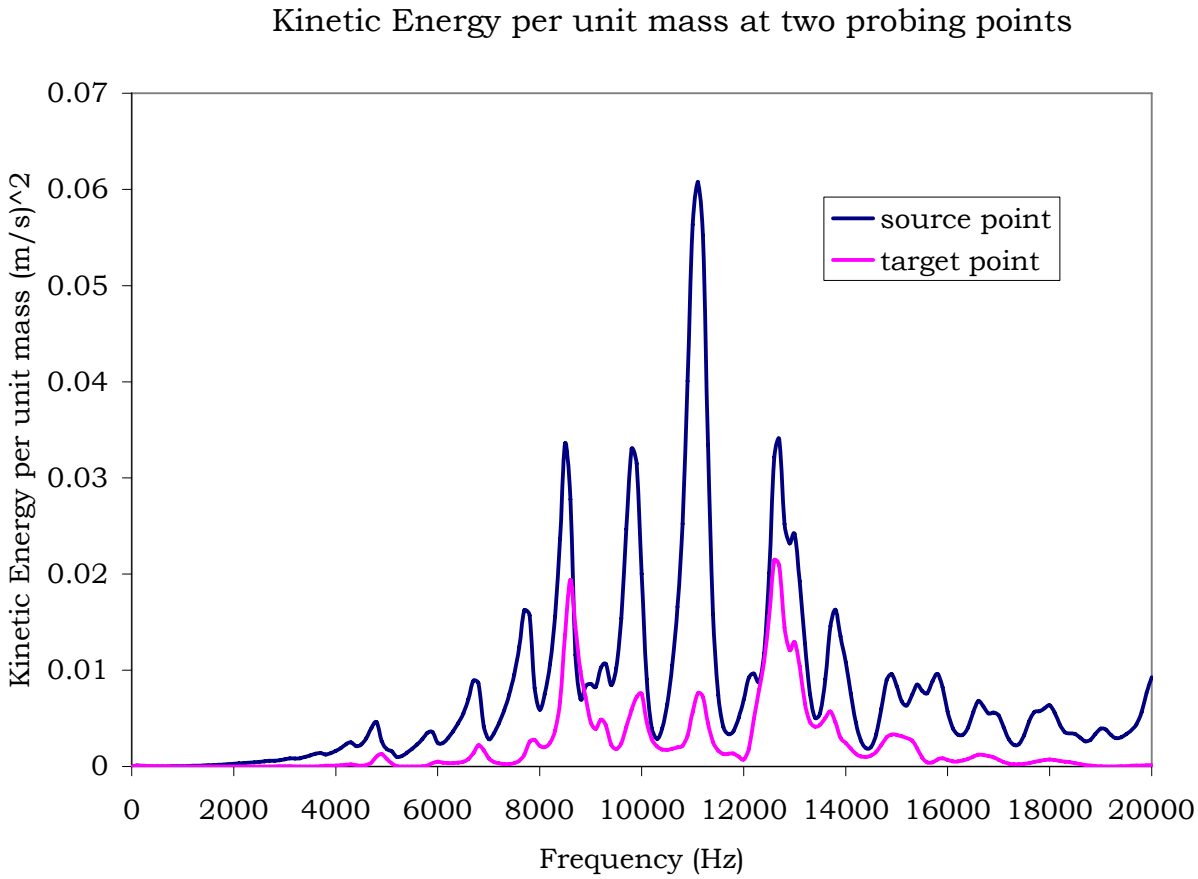

Fig. 8.2: Comparison of kinetic energy per unit mass at source and target points

Figure 8.2 demonstrates the kinetic energy level at two probing points: source and target. It is clear that the energy level at target point is very small in order of magnitude compared to that of source point.

The real value of the negative effective elastic modulus of the complex structure along x direction has been found between 7.5 kHz and 16 kHz as shown in figure 8.3. The complex structure does not show the negative complex modulus at all natural frequencies of that structure.

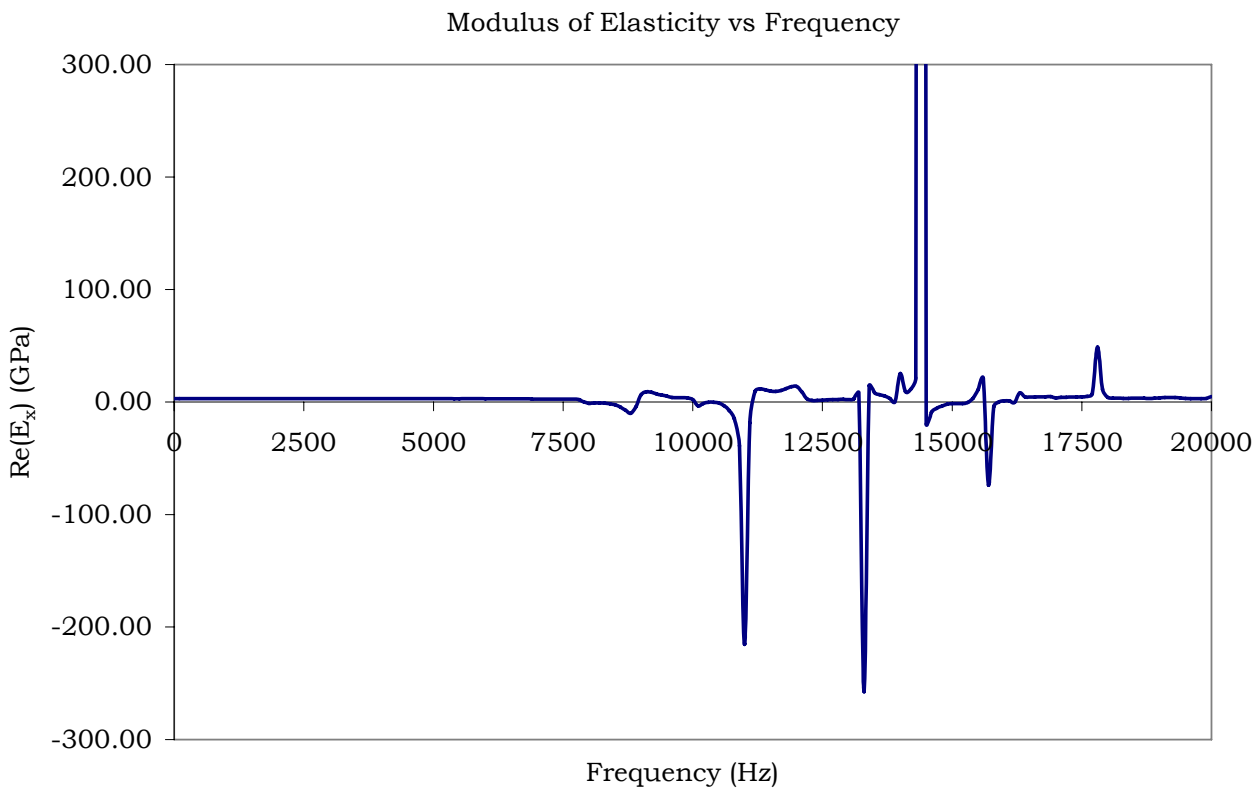

Fig. 8.3: Variation of elastic modulus of complex structure over wide range of frequencies

However, at several natural frequencies, the real values of the complex modulus become negative when the structure approaches to its resonances. This negative elastic modulus of the structure implies that the energy having tendency to pass through the system can not pass

with full energy level because the internal masses attached with stems absorb significant energy by their dynamic motion near resonances. Hence it creates energy band gap within the complex structure.

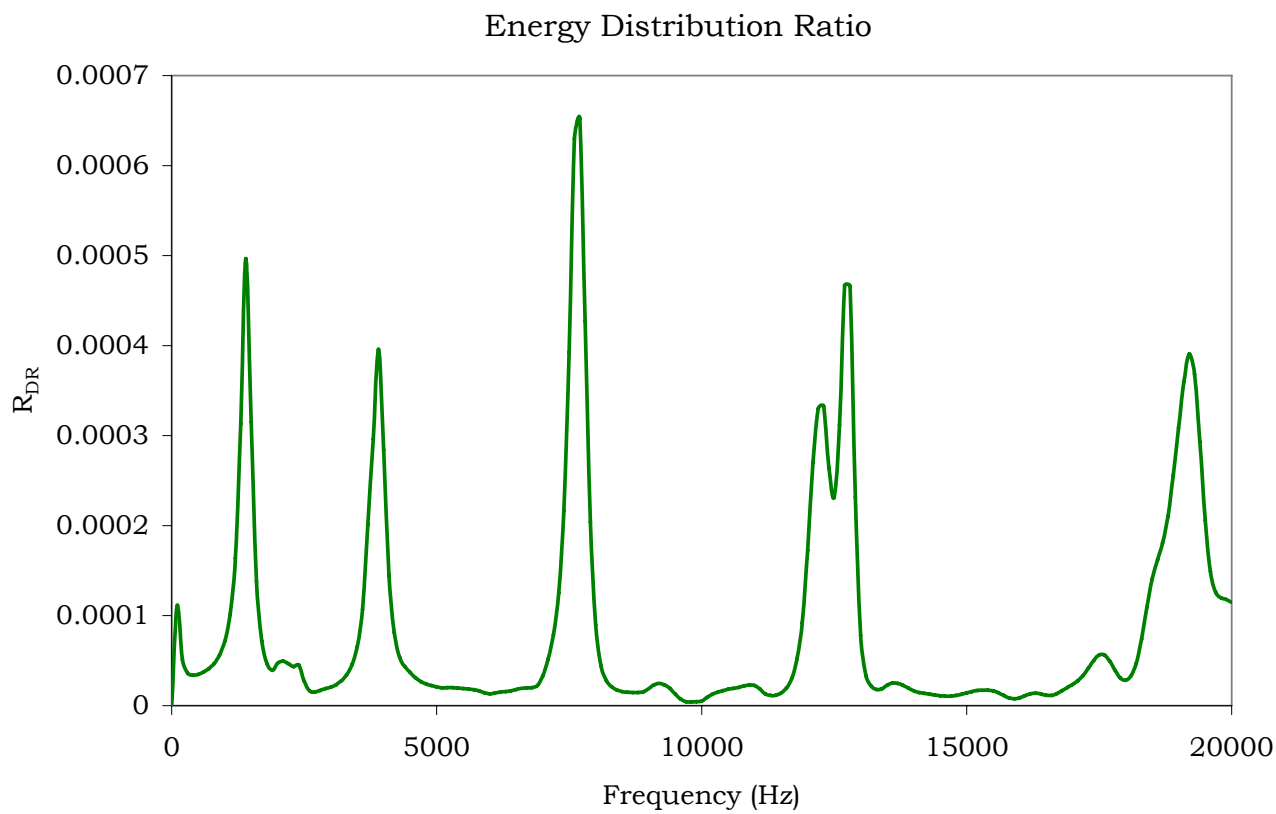

Fig. 8.4: participation of internal masses attached with stems for energy absorption

Figure 8.4 represents the ratio of kinetic energy of array of internal masses mounted on stems and the total kinetic energy of the complex system. It indicates that the participation of array of internal masses is higher near the natural frequencies of the structure. Near the natural frequencies of the structure, the work done by the external excitation is significantly transferred to kinetic motion of internal masses which in turn creates energy dipping inside the structure.

Figure 8.5 shows the surface plot of displacement along x-direction and deformation of the solid domains: internal masses with stems and acoustic cavity walls at different natural frequencies of the vibro-acoustic structure. At resonance 2300 Hz, there is small displacement of the internal masses with stems which indicates the participation of internal masses in energy absorption is initiated but little in magnitude. However, for higher resonances, the influence of internal masses in energy absorption becomes significant due to the kinetic motion of the masses with stems. This causes negative effective elastic modulus at some frequencies near the resonances of the complex structure.

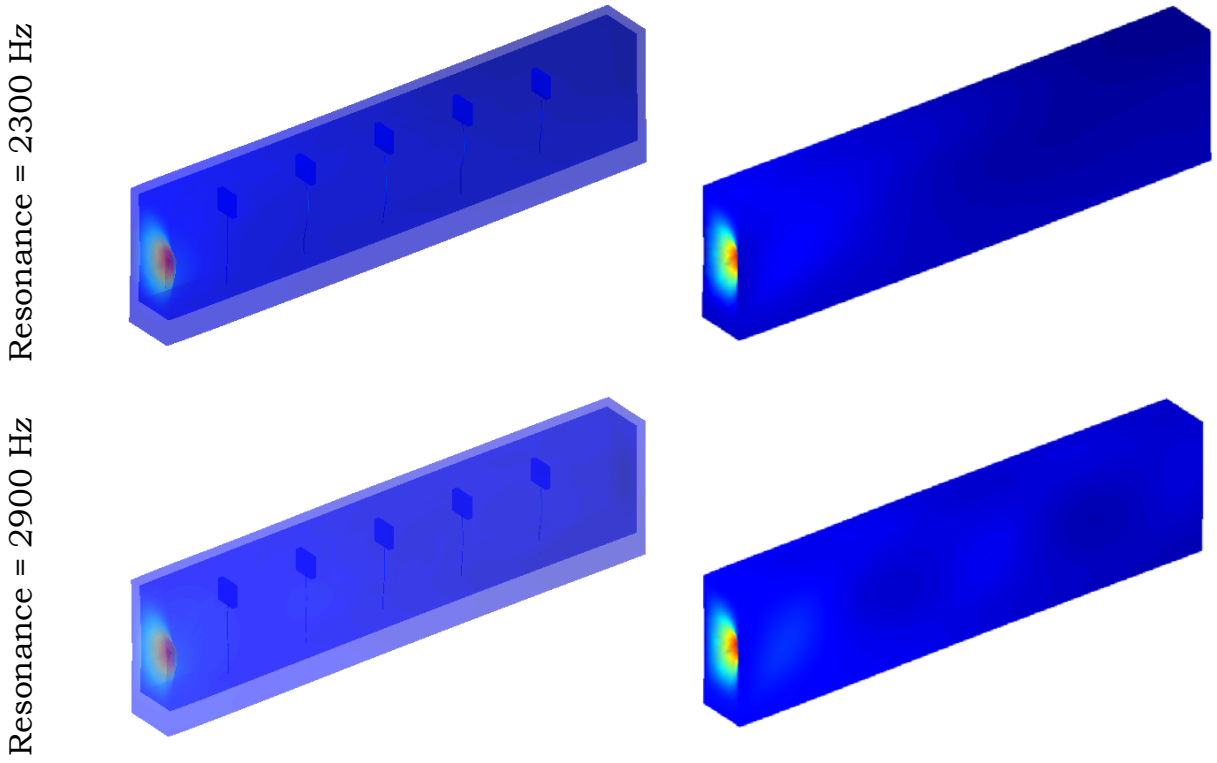

Resonance = 8000 Hz

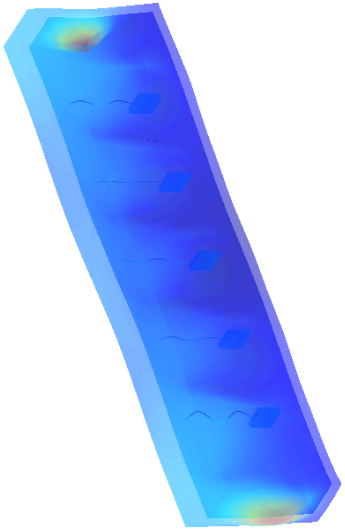

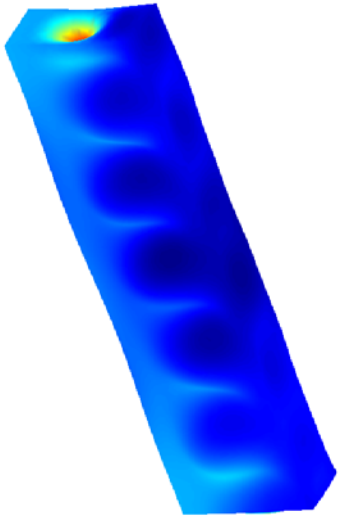

Resonance = 6900 Hz

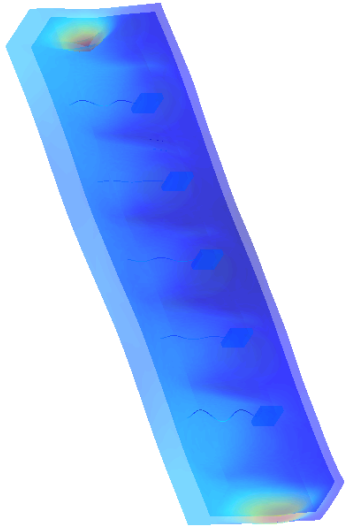

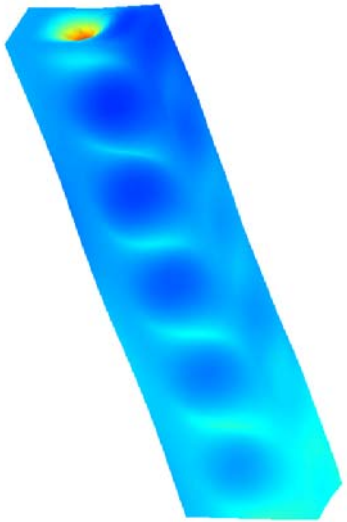

Resonance = 4900 Hz

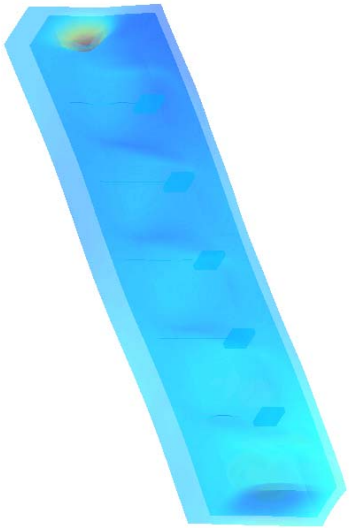

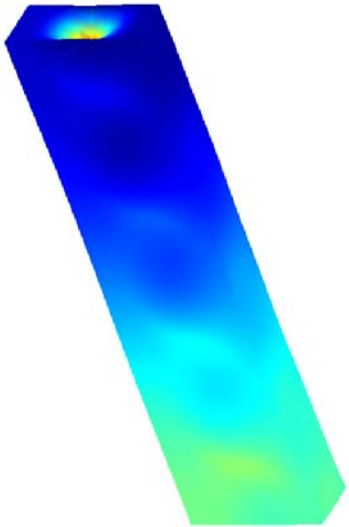

Resonance = 4300 Hz

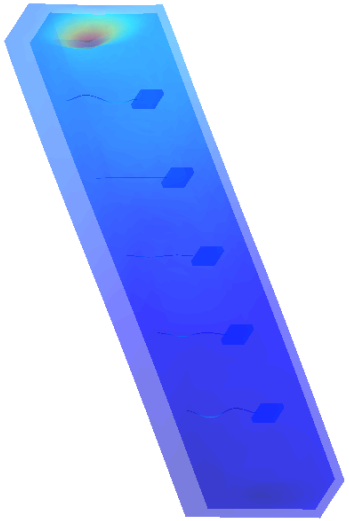

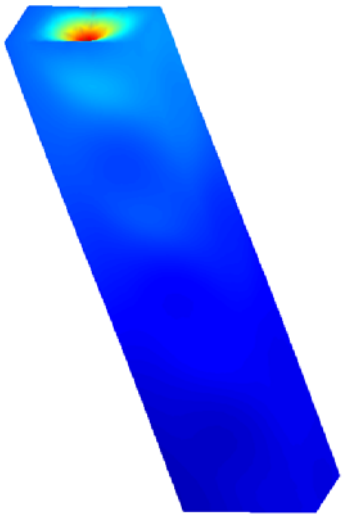

Resonance = 14800 Hz Resonance = 12600 Hz Resonance = 10300 Hz Resonance = 8800 Hz

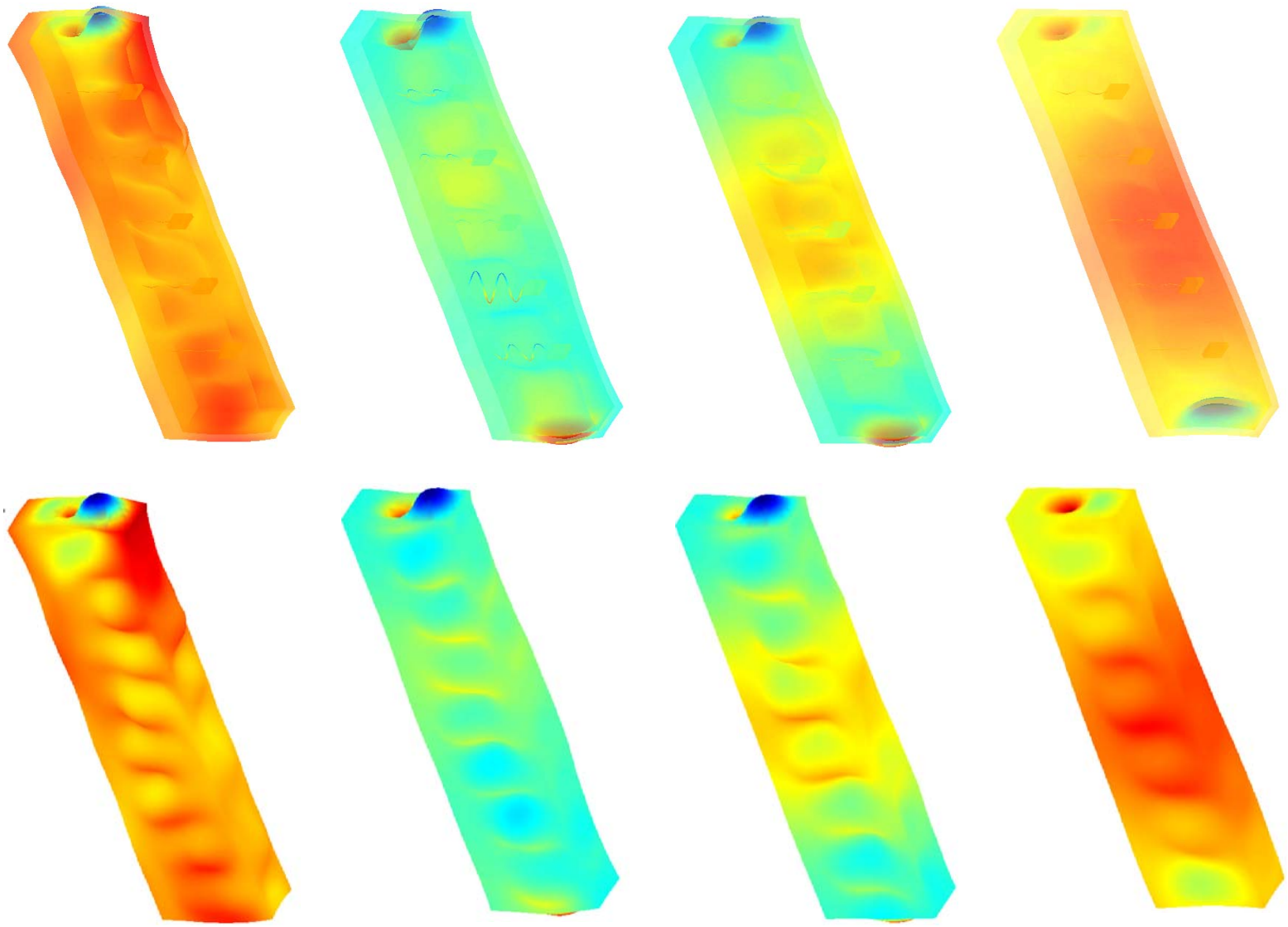

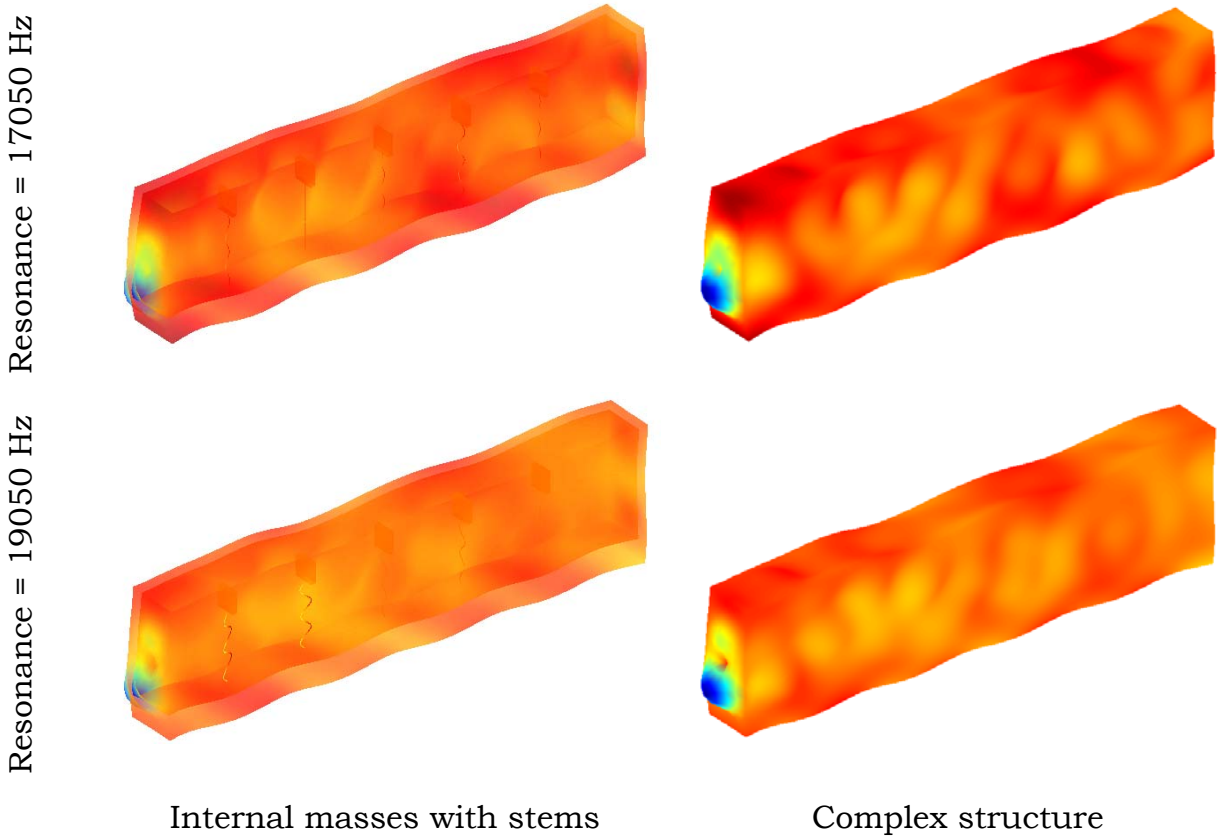

Fig. 8.5: Displacement along x-direction and deformation of internal masses with stems and complex structure

CHAPTER 9
CONCLUSION

The present research work is an effort to design and fabricate a vibro-acoustic metamaterial which can create energy dipping within the complex system by the participation of dynamic vibration of an array of internal masses attached with stems surrounded by the acoustic cavity. Eventually, it has been proven that a vibro-acoustic metamaterial with negative effective mass and negative effective elastic modulus near resonances can be created. The total energy generated by the external force is captured in a significant amount within the system by the kinetic motion of the array of internal masses attached with stems. These internal masses contribute in the energy absorption near the natural frequencies of the complex designed structure, though the contribution of the internal masses is not prominent at first few cycles. It can be noteworthy that the vibro-acoustic metamaterial has larger mass damping parameter than stiffness damping parameter. Moreover, this complex structure can create shield at more than one resonance. Therefore, the tuning of design parameter for certain frequency attenuation is not necessary.

REFERENCES

[1] Veselago, V. G., “The electrodynamics of substances with simultaneously negative values of ε and μ”, Soviet Physics Uspekhi, vol. 10 (4), pp. 509 - 514, Jan - Feb 1968

[2] Pendry, J. B., “Negative Refraction Makes a Perfect Lens”, physical Review Letters, vol. 85 (18), pp. 3966 - 3969, 30 October 2000

[3] Fang, N., Xi, D., Xu, J., Ambati, M., Srituravanich, W., Sun, C. and Zhang, X., “Ultrasonic metamaterials with negative modulus”, Nature Materials, vol. 5, pp. 452 - 456, June 2006

[4] Huang, H. H., Sun, C. T. and Huang, G. L., "On the negative effective mass density in acoustic metamaterials", Intl. J. Engineering Science, vol. 47, pp. 610 – 617, 2009

[5] Sugimoto, N. and Horioka, T., “Dispersion characteristics of sound waves in a tunnel with an array of Helmholtz resonators”, J. Acoust. Soc. Am., vol. 97 (3), pp. 1446 - 1459, March 1995

[6] Milton, G. W. and Willis, J. R., “On modifications of Newton’s second law and linear continuum elastodynamics”, Proc. R. Soc. A, vol. 463, pp. 855 - 880, 2007

[7] Cantrell, R. H. and Hart, R. W., “Interaction between Sound and Flow in Acoustic Cavities: Mass, Momentum, and Energy Considerations”, J. Acoust. Soc. Am., vol. 36 (4), pp. 697 – 706, April 1964

[8] Soize, C., “Reduced models for structures in the medium – frequency range coupled with internal acoustic cavities”, J. Acoust. Soc. Am., vol. 106 (6), pp. 3362 – 3374, December 1999

[9] Esteve, S. J. and Johnson, M. E., “Reduction of sound transmission into a circular cylindrical shell using distributed vibration absorbers and Helmholtz resonators”, J. Acoust. Soc. Am., vol. 112 (6), pp. 2840 – 2848, December 2002

[10] Hepberger, A., Pluymers, B., Jalics, K., Priebsch, H. H. and Desmet, W., “Validation of a wave based technique for the analysis of a multi – domain 3D acoustic cavity with interior damping and loudspeaker excitation”, 33rd Intl. Congress and Exposition on Noise Control Engineering, August 22 – 25, 2004

[11] Kung, C. –H. and Singh, R., “Experimental modal analysis technique for three dimensional acoustic cavities”, J. Acoust. Soc. Am., vol. 77 (2), pp. 731 – 738, February 1985

[12] Wang, X. and Bathe, K. –J., “Displacement/pressure based mixed finite element formulations for acoustic fluid – structure interaction problems”, Intl. J. Num. Meth. Engg., vol. 40, pp. 2001 – 2017, 1997

[13] Li, H., Hao, J., Zhou, L., Wei, Z., Gong, L., Chen, H. and Chan, C. T., "All-dimensional subwavelength cavities made with metamaterials", Applied Physics Letters, vol. 89, 2006

[14] Li, H., Hang, Z., Qin, Y., Wei, Z., Zhou, L., Zhang, Y., Chen, H. and Chan, C. T., "Quasi-periodic planar metamaterial substrates", Applied Physics Letters, vol. 86, 2005

[15] Genov, D. A., Zhang, S. and Zhang, X., "Mimicking celestial mechanics in metamaterials", nature physics, 20 July 2009

[16] Wu, L., Chen, L. and Liu, C., "Experimental investigation of the acoustic pressure in cavity of a two-dimensional sonic crystal", Physica B, vol. 404, pp. 1766 – 1770, 2009

[17] Wu, L., Chen, L. and Liu, C., "Acoustic pressure in cavity of variously sized two-dimensional sonic crystals with various filling fractions", Physics Letters A, vol. 373, pp. 1189 – 1195, 2009

[18] Espinosa, F. R. M., Jimenez, E. and Torres, M., "Ultrasonic Band Gap in a Periodic Two-Dimensional Composite", Physical Review Letters, vol. 80(6), pp. 1208 – 1211, 9 February 1998

[19] Hu, J., Zhou, X. and Hu, G., "A numerical method for designing acoustic cloak with arbitrary shapes", Computational Materials Science, 2009

[20] Torrent, D. and Sanchez - Dehesa, J., “Effective parameters of clusters of cylinders embedded in a nonviscous fluid or gas”, Physical Review B, vol. 74, pp. 224305-1 - 224305-10, 2006

[21] Chen, H. and Chan, C. T., "Acoustic cloaking in three dimensions using acoustic metamaterials", Applied Physics Letters, vol. 91, 2007

[22] Ambati, M., Fang, N., Sun, C. and Zhang, X., "Surface resonant states and superlensing in acoustic metamaterials", Physical Review B, vol. 75 (195447), pp. 1 – 5, 2007

[23] Zhang, S., Yin, L. and Fang, N., "Focusing Ultrasound with Acoustic Metamaterial Network", PACS numbers: 43.20.

[24] Material Property Data: www.matweb.com

[25] Goldman, S., "Vibration Spectrum Analysis: A Practical Approach", 2nd Edition, © 1999, Industrial Press Inc., New York, New York, ISBN 0-8311-3088-1

[26] Commercial FEA Software: COMSOL Multiphysics version 3.5

ABSTRACT

ANALYSIS AND EVALUATION OF A VIBRO-ACOUSTIC METAMATERIAL

by

MD TOFIQUL ISLAM

May 2011

Advisor: Professor Golam M Newaz

Major: Mechanical Engineering

Degree: Master of Science

The effects of negative effective mass density and negative effective elastic modulus on energy absorption have been investigated experimentally and numerically. It is noteworthy that the classical continuum mechanics support the concept of negative effective elastic modulus of artificially designed vibro – acoustic metamaterial. Both the negative effective mass density and the effective negative elastic modulus are frequency dependent and are shown up near the natural frequencies of the complex structure. The physical structure has been designed in such a fashion so that only longitudinal planar waves at a frequency of 0 – 20 kHz can propagate throughout the system. The free – free vibration testing has been conducted to evaluate the natural frequencies of the complex system and to determine the negative effective mass density near resonances. Moreover, the numerical platform is based on acoustic – structural interaction physics. By performing frequency analysis, the negative effective elastic modulus of the complex structure, which

demonstrates the energy absorption phenomenon, has been found numerically.

AUTOBIOGRAPHICAL STATEMENT

Md Tofiqul Islam

Educational Background:

M. S. (Mechanical Engineering, concentration - Solid Mechanics) Wayne State University, Detroit, MI 48202, USA, **GPA 4.0/4.0** *(May 2011)*

M.Sc. (Mechanical Engineering, concentration - Thermo-Fluid Mechanics) Bangladesh University of Engineering and Technology (BUET), Dhaka 1000, Bangladesh, **GPA 3.92/4.00** *(October 2007)*

B.Sc. (Mechanical Engineering) Bangladesh University of Engineering and Technology (BUET), Dhaka 1000, Bangladesh, **GPA 3.81/4.00** (**2nd in merit position out of 160 students**) *(June 2005)*

Work Experience:

- Graduate Research Assistant, Mechanical Engineering Department, Wayne State University, Detroit, MI 48202 (Aug 2009 – May 2010)
- Instructor Assistant, Institute for Manufacturing Research, Wayne State University, Detroit, MI 48202 (May 2009 - Aug 2009)
- Graduate Research Assistant, Institute for Manufacturing Research, Wayne State University, Detroit, MI 48202 (Jan 2009 - May 2009)
- Reviewer of Journal of Applied Science and Engineering Technology, Rochester Institute of Technology, College of Applied Science and Technology (Fall 2007 – present)

Recent Publications:

1. **Md. Tofiqul Islam** and Golam Newaz, "*Double Negative Vibro-Acoustics Metamaterial",* Accepted in International Symposium on Acoustic Metamaterials, Beijing, May 23-28 2011.

2. M. A. H. Mamun, **Md. T. Islam** and Md. M. Rahman, "*Natural Convection in a Porous Trapezoidal Enclosure with Magneto-hydrodynamic Effect*", Journal of Lithuanian Association of Nonlinear Analysts LANA, Vol. 15 (2), 2010.